Edisto Inlet as a sentinel for the Late Holocene environmental changes over the Ross Sea: insights from foraminifera turnover events

Giacomo Galli[1,2], Katrine Elnegaard Hansen[3], Caterina Morigi[2], Alessio di Roberto[4], Federico Giglio[5], Patrizia Giordano[5] and Karen Gariboldi[2]

[1]Department of Environmental Sciences, Informatics and Statistics, Ca' Foscari University of Venice, Via Torino 155, 30172 Venice, Italy
[2]Department of Earth Sciences, University of Pisa, Via Santa Maria 53, 56126, Pisa, Italy
[3]Department of Near Surface Land and Marine Geology, The Geological Survey of Denmark and Greenland (GEUS), 8000 Aarhus C, Aarhus, Denmark
[4]National Institute of Geophyisics and Vulcanology (INGV), Section of Pisa, Via Cesare Battisti 53, 56125, Pisa, Italy
[5]National Institute of Polar Sciences (CNR-ISP), Section of Bologna, Via Piero Gobbetti 101, 40129, Bologna, Italy

Correspondence to: Giacomo Galli (giacomo.galli@unive.it)

Abstract. Identifying ~~key~~marine environmental changes is important to understand the processes that govern the Earth's climate system and ~~all~~ its interacting components. Microfossil assemblages~~Micropaleontological proxies~~ are one of the most used ~~proxies~~paleoenvironmental tracers, being able to connect in their composition~~abundances of species~~ to changes in the physiochemical characteristics of the environment. In this context, foraminifera have been extensively used due to their preservation potential. However, little attention has been paid to the properties of the whole foraminiferal community that, in turn, can be used to depict a comprehensive view of the environment. In this study we focused on the laminated marine sediment core TR17-08 collected in the Edisto Inlet (Ross Sea, Antarctica), and the turnover events that characterized the foraminiferal fauna over the last 3.6 kyrs BP. Using the~~Using the~~ Rate-of-Change analysis (RoC) ~~analysis,~~ three distinct turnover events ~~with long term effects on the fauna were recognised~~ were recognised at 2.7-2.5 kyrs BP, at 1.2-1.0 kyrs BP and at 0.7 kyrs BP. ~~Through the analysis of the most common benthic foraminiferal species, it was possible to connect them to specific changes in the environment.~~ At 2.7-2.5 kyrs BP a change from a *Miliammina arenac* a more prominent presence of *Epistominella exigua, Nonionella iridea* and *Stainforthia feylingi* characterized this transition. Aligning with the micropaleontological interpretations, changes in XRF ratios (Zr/Rb; Ca/Ti and Br/Ti) were coeval with the interpretation derived from the RoC and the microfossils assemblage composition. Over this transition, a switch from a multi-year landfast sea-ice (3.6-2.7 kyrs BP) to a seasonal sea-ice dominated environment (2.5-1.2 kyrs BP) was driven by a change in the water mass characteristics, increasing the mCDW (modified Circumpolar Deep Water) content inside the fjord as well as ~~increase~~ the duration of summer ice-free period. Higher RoC values suggested the absence of a stable benthic foraminifera community ~~over~~ the multi-year landfast sea-ice scenario, while lowest RoC values ~~over~~ the seasonal sea-ice phase are present, especially ~~over~~ the 2-1.5 kyrs BP interval, aligning with the macrofaunal response inside the inlet.~~In addition, by comparing the TR17-08 records with other proxies~~ Continental archives (Penguin and Elephant Seals remains) ~~over~~ the Victoria Land Coast reported ~~this~~ change in the sea-ice type ~~over~~ the Late Holocene. This study provides further evidence of a change in the sea-ice state ~~over~~ the Ross Sea after 2.7-2.5 kyrs BP thus providing further evidence that ~~this~~ water mass intrusion ~~inside~~ the continental

shelf ~~were higher~~ over the 2.5 – 1.2 kyrs BP period, in accordance with persistent summer positive mode of the Southern Annular Mode. Lastly, this study highlights that using ecological properties of the benthic foraminifera community can be a valuable source of information for high-resolution studies and can provide additional insights into the paleoenvironmental interpretation and paleoclimatic reconstruction that uses benthic foraminiferal species as environmental indicators. ~~from nearby cores we identify a switch from a multi-year landfast ice (3.5-2.7 kyrs BP) to a seasonal sea-ice dominated environment (2.5-1.5 kyrs BP). Other Victoria Land Coast sites reported this change in the sea-ice type over the Late Holocene, suggesting that the increase in the seasonal sea-ice environment is connected to entrance of mCDW. Our study also suggests an increase in the presence of mCDW in the fjord after 2.7-2.5 kyrs BP. Lastly, the presence of expanded laminated sequence at the bottom of the Inlet makes this site an exceptional record for studying the evolution of the Late Holocene environmental conditions over the Ross Sea.~~

1 Introduction

Unveiling past environmental changes is fundamental to understand processes that governs the Earth's climate system, and it helps to pinpoint its behaviour in the future. To investigate the past environment, different proxies have been used to obtain a holistic view of all the interacting compartments of the climate system (Strugnell et al., 2022; Toyos et al., 2020; Wang et al., 2023; Wu et al., 2020; Yokoyama et al., 2016). In marine settings, a~~A~~ group that has been extensively used as a tracer for environmental changes are ~~the~~ benthic and planktic foraminifera: unicellular marine eukaryotes, with different test material that have a great preservation potential (Sen Gupta, 2003; Murray, 1991, 2006). These organisms inhabit both the surface and bottom water, and they can be used to infer changes in the paleoenvironmental evolution of an area (Sen Gupta, 2003; Murray, 1991, 2006). However, most of the studies that have been carried out with foraminifera focus on comparing changes in the relative abundances of a single species or a group of species and connect them to specific changes in the environment (i.e., Ishman & Sperling, 2002).

~~In this context, understanding the Late Holocene period is extremely important due to the succession of different climate phases that can be related to present and future climate scenarios. Thus, using more ecological proxies can be fundamental to disentangle the complex interactions between the physical environment and the biota.~~

Community-level (i.e., the whole assemblage considered as one indivisible unit) analysis can help us understand the effects of different environmental phases on the local fauna, while also providing key insight into the environmental evolution (Foster et al., 1990). Little to no attention has been paid to the properties of the whole community that, potentially, can be used as a reliable proxy to identify significant turnover events linked to the succession of different environmental phases (Hansen et al., 2023; Tomašových and Kidwell, 2010)

The *Rate-of-Change* (RoC) analysis ~~can be used to infer changes at the community level~~calculates the compositional change of a given community through time to extrapolate the rate at wich, ~~hence the~~looking at how the whole community is changing. ~~through time~~. This can be used to infer statistically significant changes in the assemblage composition, the so-called Turnover

Events (TEs) (Foster et al., 1990; Hansen et al., 2023; Jacobson and Grimm, 1986; Mottl et al., 2021b, a; Shimadzu et al., 2015). The analysis was used by Hansen et al. (2023) on the ecological traits of the benthic foraminifera to infer ecological responses over the western coast of Greenland. This was crucial to understand the consequences of the deglacial-Holocene and
70 the Mid-Holocene warming on the benthic foraminifera fauna in the area, while simultaneously showing that significant TEs can be linked to significant climatic perturbation.

In this study, we analysed the marine sediment core TR17-08 from Edisto Inlet (Victoria Land, Antarctica, Fig. 1) with the purpose of understanding short-term (centennial) and long-term (millennial) environmental changes in the area and how they connect with faunal turnover events.

75 Edisto Inlet is a small basin (16 km long, 4 km ~~located~~wide) located on the northern tip of the Victoria Land in the Ross Sea, characterized by a 110-m thick laminated sedimentary sequence on the bottom, spanning the entire Holocene (Battaglia et al., 2024; Finocchiaro et al., 2005; Di Roberto et al., 2023; Tesi et al., 2020). Previous studies conducted in the inlet have highlighted environmental changes occurred over the Late Holocene linked to changes in the global climatic system: the Medieval Climate Anomaly (MCA, ca. 1.5 kyrs BP) and the Little Ice Age (LIA, ca. 0.7 kyrs BP) (Galli et al., 2023, 2024;
80 Lüning et al., 2019; Mezgec et al., 2017; Stenni et al., 2017; Tesi et al., 2020). In addition, the study of Galli et al., (2024) on ophiuroid ossicles in conjunction with the diversity of the foraminiferal assemblages (Fig. 1c), proposed a shift from an unstable seasonal sea-ice cycle (3.6 – 2.5 kyrs BP) to a stable sea-ice cycle (2.5-1.5 kyrs BP), with an optimum of this environmental condition from 2 to 1.5 kyrs BP. The latter has been regarded as the "Ophiuroid Optimum" because of the increase in the probability of occurrence of the ophiuroid *Ophionotus victoriae*, the lowest values of the $IPSO_{25}$ from the
85 HLF17-01 (Fig. 1c)The transition centred at 2.5 kyrs BP is characterized by a stepwise decrease in the flux and quantity of organic matter content, as testified by the reduction of the Benthic and Planktic Foraminifera Accumulation Rate (BFAR and PFAR, respectively) and by a decrease in the Ice Rafted Debris (IRD) content that suggested the presence of the seasonal sea-ice cover ~~over~~ this period.

~~Moreover, the position of the Edisto Inlet (Fig. 1), makes it a suitable area to study the past response of the local glaciers and~~
90 ~~the regional oceanographic conditions to climate perturbations, as well as their interactions. This enables a better understanding~~
~~of the types of changes influencing the local benthic foraminiferal fauna.~~

In Edisto Inlet, t~~The~~ depositional regime ~~of the inlet~~ is governed by the seasonal cycles of landfast sea-ice, a particular type of sea-ice that forms through the freezing of the seawater and by remaining attached to the coast (Fraser et al., 2023). This seasonal behaviour produces the lamination pattern, relating it to the austral summer depositional setting. The first break up of the fjord
95 sea-ice cover happens at the beginning of the austral spring season and leads to the deposition of a dark lamina (Tesi et al., 2020). This type of lamina is characterised by a diatom assemblage dominated by the *Fragilariopsis* genus. Prolonged periods of ice-free scenarios lead to the deposition of a white laminae, which are dominated by the diatom *Corethron pennatum*, indicating an oligotrophisation of the upper water column (Tesi et al., 2020). This is also reflected in the biomarker $IPSO_{25}$ (Belt et al., 2016). This geochemical proxy is produced by diatom's that lives inside the sea-ice (sympagic), which is released
100 upon the first break up of the sea-ice. Due to the dependency of the sea-ice presence of sympagic diatoms to thrive, lower

IPSO$_{25}$ concentration have been connected to prolonged period with an absence of a sea-ice cover (Belt et al., 2016; Massé et al., 2011; Tesi et al., 2020). Hence, dark laminae have a higher concentration of this biomarker than light ones.

Also, previous studies conducted in the Edisto Inlet have highlighted that several environmental changes occurred over the Late Holocene linked to changes in the global climatic system: the Medieval Climate Anomaly (MCA, ca. 1.5 kyrs BP) and the Little Ice Age (LIA, ca. 0.7 kyrs BP) (Galli et al., 2023, 2024; Lüning et al., 2019; Mezgec et al., 2017; Stenni et al., 2017; Tesi et al., 2020).

Since most of the depositional signal in the fjord is dominated by the summer season, if this pervious interpretation of an unstable-to-stable transition occurred, then the rate at which the benthic community is shifting should be higher before the transition, reflecting a period in which a stable community cannot form. In addition, we integrate the results of the RoC with the X-Ray Fluorescence (XRF) over the last 3.6 kyrs BP, focusing on the 2.5 kyrs BP transition to disentangle the environmental evolution of the area between these two different states.

Thus, the aim of this study is two-fold: 1) connecting the presence of TEs with the presence of significant environmental shifts in the area and, by doing so, unlocking a new objective way of analysing benthic foraminiferal community and and, 2) reconstructing the paleoenvironmental evolution over this 2.5 kyrs BP transition e Late Holocene to understand the relationship between local and regional changes over the study area.

1.1 ~~Ross Sea oceanography~~Study area

The Ross Sea oceanographic circulation is density driven (Fig. 1b):. tThe Antarctic Circumpolar Slope Current (ASCC) sits on top of the warmer Circumpolar current (CDW), and both flows westward along the slope. (Orsi and Wiederwohl, 2009; Smith et al., 2012; Whitworth and Orsi, 2006). The CDW can enter the continental shelf when it interacts with the saltier water masses that are flowing from the continent to the open ocean, by reducing the inclination of the isopycnal (Fig. 1 b; Budillon et al., 2011; Castagno et al., 2017; Smith et al., 2012). This modified water mass (modified Circumpolar Deep Water, mCDW) enters the continental shelf where it flows southwards, through bathymetric lows (Fig. 1b) (Dinniman et al., 2011; Wang et al., 2023). At the shelf, the inflow of the warmer water masses sustains large persistent ice-free areas, the polynyas (Mathiot et al., 2012; Rusciano et al., 2013). At this point the warm water mass lost its heat and subsides due to the increase in density by salt-rejection processes. As the sea-ice polynya forms over the area, katabatic winds move the newly formed sea-ice away from the continent, thus sustaining both the production of the sea-ice, by cooling the sea surface, and the ice-free area (Dale et al., 2017; Drucker et al., 2011). The subsided water mass form the High Salinity Shelf Water (HSSW), which flows along the same bathymetric lows as the mCDW and arrives at the shelf margin, where it cascades on the seafloor, forming the Antarctic Bottom Water (AABW) (Fig. 1b; Orsi & Wiederwohl, 2009; Wang et al., 2023; Whitworth & Orsi, 2006). Lastly, by studying the current activity in the western part of the Ross Sea, over the Drygalski througharea, it has been noted that the mCDW inflow is mostly seasonal and happens during the austral summer period (Castagno et al., 2017, Wang et al., 2023, Wang et al., 2023).
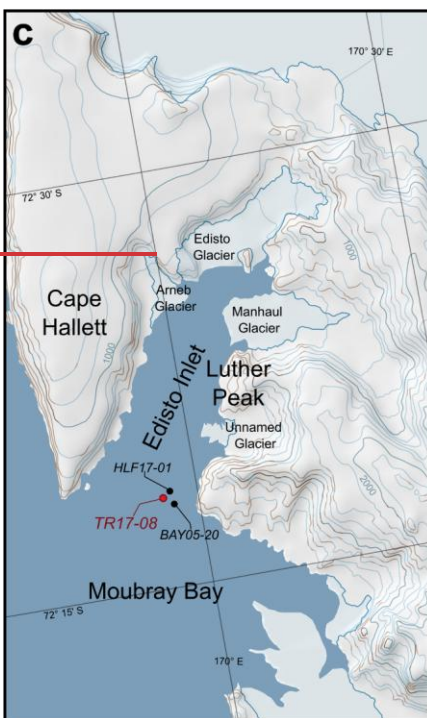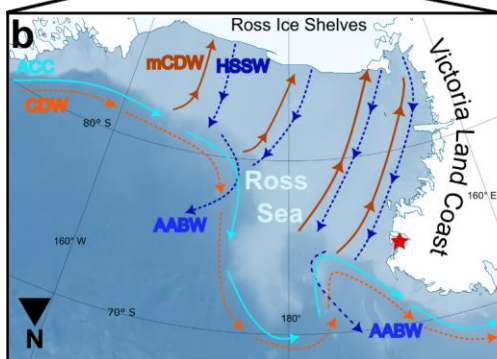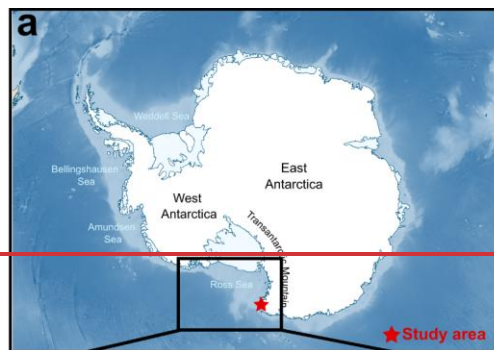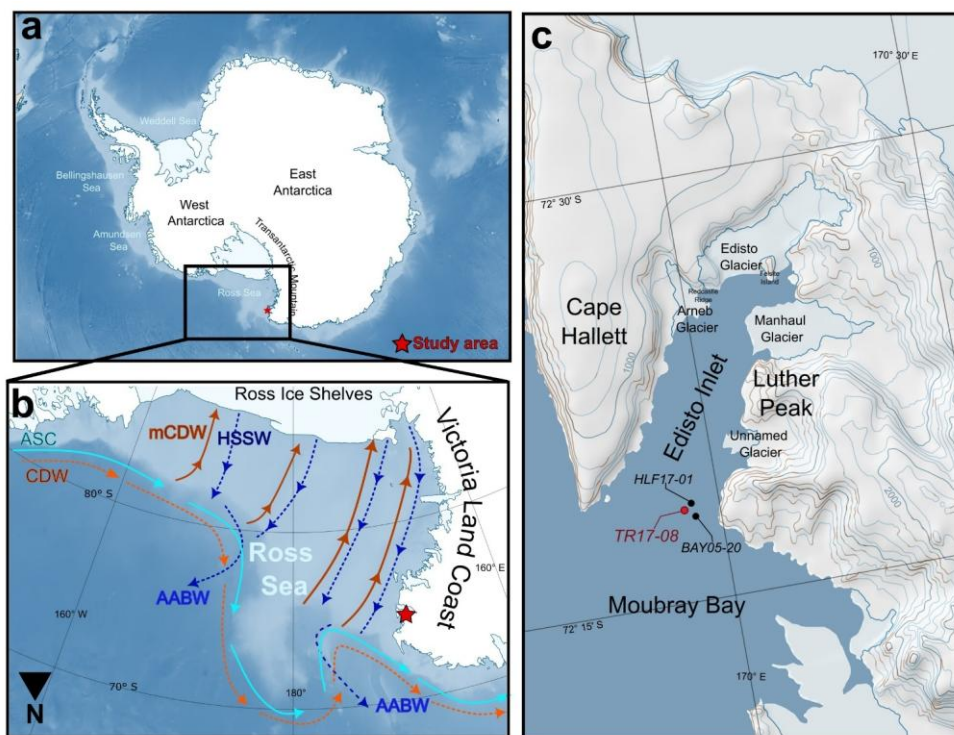
Figure 1.Simplified maps of the study area. a) The location of the study area in Antarctica (red star). b) Main oceanic currents:
ASPCC = Antarctic Slope CurrentCircumpolar current; CDW = Circumpolar Deep Water; mCDW = modified Circumpolar Deep
Water; HSSW = High Salinity Shelf Water and AABW = Antarctic Bottom Water. Red colour arrows indicate relatively warm
water masses while the cold colour ones indicate the relatively cold-water masses. Solid lines indicate surface water masses, while
the dashed ones indicate deeper water masses. The star marks the location of Edisto Inlet. c) Map of Edisto Inlet with analysed
marine sediment cores mentioned in this study marked with dots: in red the marine sediment core TR17-08 (this study), while in
black the HLF17-01 (Tesi et al., 2020) and the BAY05-20 (Mezgec et al., 2017). The maps are constructed using Quantarctica
(Matsuoka et al., 2021).

1.2 Study area

In particular, Edisto Inlet hasis a small fjord (16 km long, 4 km wide) located in the northern part of the Victoria Land Coast
in the western Ross Sea (Fig. 1c). With an an average water depth of 500 m, and the basin is defined by a sill at 400 m depth
located at the mouth that divides it from the adjacent Moubray Bay (Fig. 1c). The system is governed by seasonal cycles of
landfast sea-ice: it forms and covers the inlet over the austral winter. Afterwards, over the spring, the ice melts, and

~~consequently open water conditions prevail.~~ Moreover, four local marine terminating glaciers are present: the Arneb Glacier, the Edisto Glacier, the Manhaul Glacier and an unnamed glacier located near the mouth (Fig. 1c).

150 Oceanographic data and CTD profiles _from_~~on~~ the inner part of the fjord have shown the presence of a double layer stratification of the water column with a pycnocline/thermocline/halocline present at 50-150 m water depth (Battaglia et al., 2024). The surface layer is fresher and warmer than the deeper one (< -1.8°C). Spatially, the surface waters are saltier (34.27 PSU) and colder (-1.6°C) in the inner part of the fjord _respect to the outer ones_ (Battaglia et al., 2024).

In addition, the presence of sediment drifts at the bottom suggests the presence of relatively long-lived regular bottom water
155 circulation starting at 8 kyrs BP (Battaglia et al., 2024; Finocchiaro et al., 2005).

However, oceanographical data are scarce and for further and more detailed information about the geological and physical settings of the fjord, readers are referred to Battaglia et al., (2024).

2 Methods

~~**2.1 Core collection and dating**~~

160 To investigate the paleoenvironmental evolution of the Edisto Inlet, the piston marine sediment core TR17-08 (72° 18.2778′ S; 170° 04.1784′ E; 462 m water depth) was retrieved during the XXXII PNRA _(National Italian Program for Antarctic Research)_ scientific expedition (2016-2017) in the framework of the PNRA project TRACERS (PNRA16_00055). The core, with a length of about 14._5_~~6~~ m, is composed of diatomaceous ooze, with clear distinction between light and dark lamina (Galli et al., 2023, Fig. S1~~).~~ _.). The age-depth model used is the one proposed by Di Roberto et al., 2023 (More information about the_
165 _age-depth model in the Supplementary Material). The bottom of the core was dated around 3.6 kyrs BP, with an average sedimentation rate of 0.5 cm/yr from 3.6 to 0.7 kyrs BP. Over the last 0.7 kyrs BP, the sedimentation rate diminishes of an order of magnitude, with an average of 0.07 cm/yrs (Di Roberto et al., 2023). Foraminiferal assemblage data, Benthic and Planktic Foraminifera Accumulation Rate (BFAR and PFAR, respectively) as well as IRD (>1 mm) fluxes were used in previous studies to analyse the environmental evolution of the last 2 kyrs BP, as well as to the test the possibilities to use the_
170 _macrofaunal remains to detect stable environmental conditions (Galli et al., 2023; Galli et al., 2024). Briefly, BFAR and PFAR have been extensively used to detect changes in the organic matter flux to the bottom and the primary productivity regime, respectively (Herguera and Berger, 1991). The IRD flux have been associated to different glacial discharging regime as well as different sea-ice cover regimes, with lower values reflecting less glacial discharge and the presence of a sea-ice cover (Christ et al., 2015; Reeh et al., 1999; Zhou et al., 2021). In this study, we extend the interpretation of the environmental evolution of_
175 _this area using the micropaleontological data collected by Galli et al., (2024)._
~~The age-depth model was constructed with a Bayesian approach (OxCal. v4.4.4) and the Marine-13 calibration curve using 1 tephra layer, related to the Mount Rittman explosion (687 ± 7 years BP), and 10 other radiocarbon dated samples (Fig. 2, Di Roberto et al., 2023). A marine reservoir correction (ΔR) of 791 ± 121 yrs BP was applied according to previous studies in the area (Di Roberto et al., 2023; More information in the Supplementary material Tesi et al., 2020).~~

180 The bottom of the core was dated to around 3.6 kyrs BP, with an average sedimentation rate of 0.47 cm/yr from 3.6 kyrs BP until 0.7 kyrs BP. From 0.7 kyrs BP to present days, the sedimentation rate diminishes of an order of magnitude, with an average of 0.07 cm/yrs, in accordance with other studies in the region (Fig. 2, Tesi et al., 2020; Di Roberto et al., 2023). From 0.7 kyrs BP to present days, the sedimentation rate diminishes of an order of magnitude, with an average of 0.07 cm/yrs, in accordance with other studies in the region (Fig. 2, Tesi et al., 2020; Di Roberto et al., 2023). For more information related

185 to the age model, readers are referred to the work of Di Roberto et al. (2023).
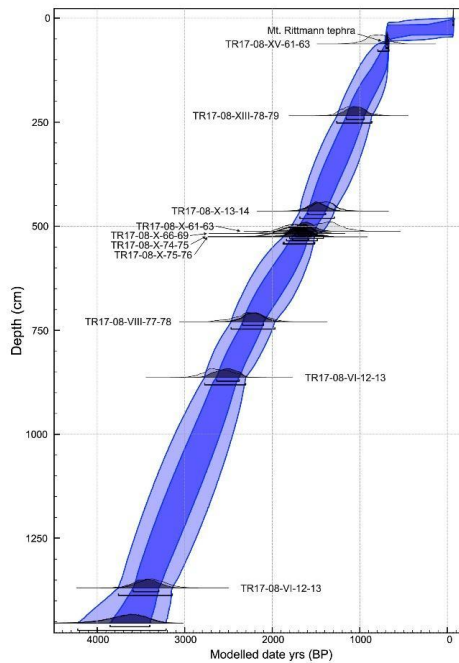
Figure 2. Bayesan age-depth model of the marine sediment core TR17-08. In dark blue is reported the 68.5% confidence interval. In light blue the 95%. Notice the almost linear sedimentation rate until 700 yrs BP (ca. 50 cm). From 700 yrs BP to present day the sedimentation rate is one order of magnitude less than the previous interval *(From di Roberto et al., 2023).*

190 **2.2 Micropaleontological samples**

One cm thick samples were collected at a sampling step of 10 cm through the core until the shift of the sedimentation rate at

0.7 kyrs BP. From 0.7 kyrs BP to the top, the sample resolution was increased down to every 5 cm to account for the change

~~in the sedimentation regime (n=152, Galli et al., 2023). Samples were washed and sieved with a mesh size of 63 μm with distilled water and the larger fraction was collected and dried overnight at 40°C. A further round of sieving was carried out at 150 μm and 1 mm. Picking was carried out on the > 150 μm fraction for every sample. All specimens were picked and identified at the lowest possible taxonomic level and collected in micropaleontological slides. Identification was done following the descriptions in Loeblich & Tappan (1988) and other previous studies conducted in Antarctica (Anderson, 1975; Capotondi et al., 2018, 2020; Igarashi et al., 2001; Ishman and Sperling, 2002; Ishman and Szymcek, 2003; Majewski et al., 2018; Violanti, 2000).~~

~~Accumulation Rates of the Benthic (BFAR) and Planktic Foraminifera (PFAR) were calculated using the following equation: $AR_t = C_t \cdot \rho_t \cdot S_t$, where C is the number of individuals per gram of dry sediments (n/g), ρ is the dry sediment density (g/cm³) and S is the sedimentation rate (cm/yr) of the i-th considered level (Herguera & Berger, 1991).~~

~~(Christ et al., 2015; Reeh et al., 1999; Zhou et al., 2021)~~

2.1~~3~~ ~~Statistical~~ Benthic foraminifera analysis

A TE can be defined as a drastic change in the species composition of a defined area (O'Sullivan et al., 2021; Shimadzu et al., 2015). Over extended periods, TEs can be linked to significant changes in the environmental conditions, providing insights into the extent to which environmental shift can impact a given ecological community, in this case the benthic foraminifera (Foster et al., 1990; Hansen et al., 2023; Mottl et al., 2021b, a). To assess how the evolution of the environment was affecting the benthic foraminiferal community, we computed and analysed the Rate-of-Change curve (RoC) derived from the relative abundances of the benthic species.

The RoC analysis is a statistical method that computes the significance of a turnover events (TE) in a palaeoecological temporal series in relation to the rate at which the community is changing (Hansen et al., 2023; Jacobson and Grimm, 1986; Mottl et al., 2021b). The analysis is based on the concept of calculating the differences between adjacent stratigraphic levels to identify significant changes in time of the shifts in the biological community (Mottl et al., 2021b, a). This significant changes in time can be detected with several methods: with a linear trend, a nonlinear trend, with the first derivative of the curve or with signal to noise ratio (Mottl et al., 2021). In our study we choose to compare significant peaks detected by using the nonlinear trend (recommended for paleoecological temporal series) and the significant departure from 0 of the first derivative of the curve (Mottl et al., 2021). The first method identifies significant turnover events if a point exceeds a 1.5 standard deviation threshold derived from a fitted non-linear trend (TnL). The second method is based on the first derivative of a fitted Generative Additive Model (GAM derivative method, Gd). The Gd detects a cluster of peaks when the first derivative of a fitted GAM of the RoC curve is significantly below 0, and it could be used to represent the outcome of a TE (Mottl et al., 2021b, a; Simpson, 2018). These detection methods can be used to infer significant TEs in a robust way since TnL and Gd are complementary in respect of what they detect (Fig. 2).

Formattato: Normale

~~To assess how the evolution of the environment was affecting the benthic foraminiferal community we computed and analysed the Rate-of-Change curve (RoC) derived from the relative abundances of the benthic species.~~

~~The RoC analysis is a statistical method that computes the significance of a turnover events (TE) in a palaeoecological temporal series in relation to the rate at which the community is changing (Hansen et al., 2023; Jacobson and Grimm, 1986; Mottl et al., 2021b). The analysis is based on the concept of calculating the differences between adjacent stratigraphic levels to identify significant changes in time of the shifts in the biological community (Mottl et al., 2021b, a). This significant changes in time can be detected with several methods: with a linear trend, a nonlinear trend, with the first derivative of the curve or with signal to noise ratio (Mottl et al., 2021). In our study we choose to compare significant peaks detected by using the nonlinear trend (recommended for paleoecological temporal series) and the significant departure from 0 of the first derivative of the curve (Mottl et al., 2021). The first method identifies significant turnover events if a point exceeds a 1.5 standard deviation threshold derived from a fitted non-linear trend (TnL). The second method is based on the first derivative of a fitted Generative Additive Model (GAM derivative method, Gd). The Gd detects a cluster of peaks when the first derivative of a fitted GAM of the RoC curve is significantly below 0, and it could be used to represent the outcome of a TE (Mottl et al., 2021b, a; Simpson, 2018). These detection methods can be used to infer significant TEs in a robust way since TnL and Gd are complementary in respect of what they detect (Fig. 2).~~

The RoC analysis was performed using the *R-Ratepool* package in R using a randomization factor of 10'000, with the recommended setup described in Mottl et al., (2021b). To account for the temporal resolution, we changed the "time standardisation" parameter to 100 and the window set to 5 to have a similar resolution between the analysis and the sample step of the core (RoC is performed every 20 years). To create the bins used to calculate the differences in the assemblages, we used the "binning with a moving window" approach as described and recommended in Mottl et al. (2021b). To better display the trends of the RoC curve a GAM model (algorithm: REML) was fitted using the *mgcv* package (Simpson, 2018; Wood Simon, 2001).

In addition to analysing the whole period, we also performed the analysis on the 0.7 – 3.6 kyrs BP period, due to the presence of a substantial change in the sedimentation rate and almost absence of foraminiferal tests from 0.7 kyrs BP to recent days (Galli et al., 2023; Di Roberto et al., 2019).
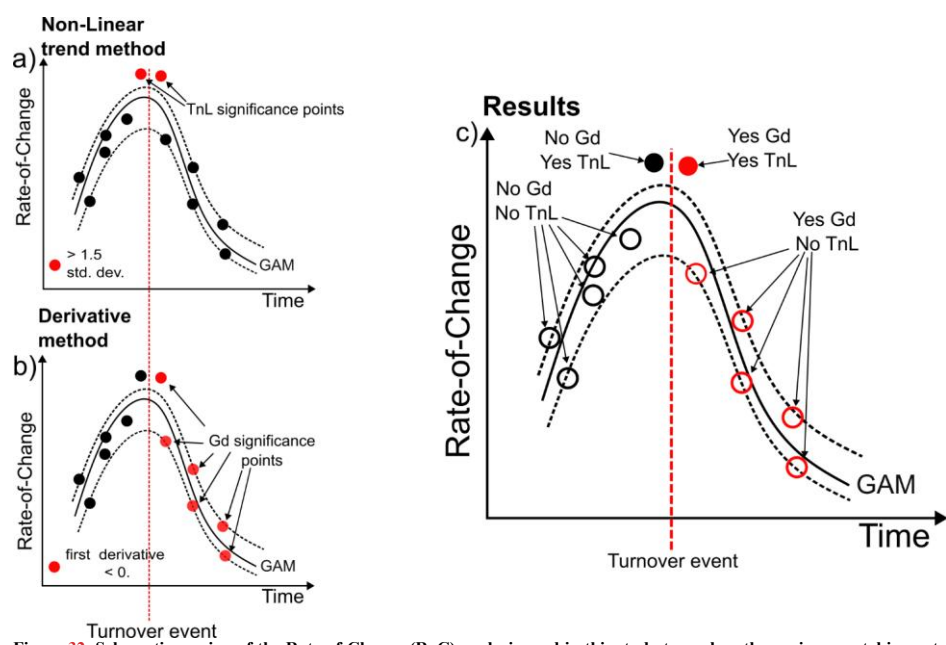
Figure ~~3~~2. Schematic version of the Rate-of-Change (RoC) analysis used in this study to analyse the environmental impact on the foraminiferal community. a) Non-linear trend detection method (TnL) that relies on points > 1.5 std. dev. of a fitted non-linear trend. b) GAM derivative method (Gd) that relies on the first derivative being < 0. c) End results of the analysis when combined the TnL and the Gd significance points. In this conceptual example, the Turnover Event (red dotted line) is represented as an instantaneous event.

~~The red dotted line indicates a hypothetical turnover event.~~

2.4 Sediment properties and lithology

To reconstruct the changes in the sedimentary depositional environment of the study area, a third generation AVAATECH core scanner was used to acquire high-resolution ~~X-Ray Fluorescence~~ (XRF~~)~~ data at 1 cm intervals at the Institute of Marine Sciences at the Italian National Research Council (CNR-ISMAR) of Bologna. The base-10 logarithm of Zr/Rb, Br/Ti and Ca/Ti as used to interpret sedimentary, environmental, and climatic processes suggested by Croudace & Rothwell (2015). The Zr/Rb ratio have been used to track changes in the mean-grain size of the silt fraction that can be linked to current strength, with high values reflecting a high current dynamic (Lamy et al., 2024; Wu et al., 2019, 2020).

Br/Ti ratio can be used as proxy for the primary productivity, since Br is related to organic matter of marine origin (Wu et al., 2019; Ziegler et al., 2008)~~., and~~ Ca/Ti has been used to infer changing in the biogenic vs. lithogenic sedimentation due to the more prominent presence of Ti in the detrital material than the marine counterpart and Ca mostly derived from biogenic mineralization (Piva et al., 2008; Taylor et al., 2022). ~~and Ca mostly derived from biogenic mineralization (Piva et al., 2008; Taylor et al., 2022).~~ To reduce the noise of these temporal series, a LOESS smoothing curve with a narrow smoothing window (λ=0.1) was fitted using the function *lm* of the base version of R (R Core Team, 2023)~~,~~

~~A LOESS smoothing curve with a narrow smoothing window (λ=0.1) was fitted to reduce the noise of the time series using the software R (R Core Team, 2023).~~

~~Angular clasts collected from the sieved > 1 mm fraction were regarded as Ice Rafted Debris (IRD) and the accumulation rates were calculated using the equation from section 2.2.~~

~~The IRD content can be used to infer changes in the glacial proximity and in the seasonal sea-ice cover (Christ et al., 2015; Galli et al., 2024; Reeh et al., 1999; Zhou et al., 2021). Higher values of this parameter can be used to infer an increase in the glacial proximity, while lower values can be connected to non-glacial activity or the presence a seasonal sea-ice cover.~~

3 Results and discussion

3.1 Turnover events over the last 3.6 kyrs BP in ~~the~~ Edisto Inlet

~~A total of 51 foraminifera were recognised, of which only one species was planktic (*Neogloboquadrina pachyderma*). The complete taxonomical list is reported in the supplementary material (Table S1).~~

Turnover Events (TEs) were defined only over the benthic foraminiferal community due to the presence of only one planktic species.

~~A TE can be defined as a drastic change in the species composition of a defined area (O'Sullivan et al., 2021; Shimadzu et al., 2015). Over extended periods, TEs can be linked to significant changes in the environmental conditions, providing insights into the extent to which environmental shift can impact a given ecological community, in this case the benthic foraminifera (Foster et al., 1990; Hansen et al., 2023; Mottl et al., 2021b, a).~~

The RoC computed for the species composition shows some significant Gd clusters starting at 3.3 kyrs BP, 2.5 kyrs BP and at 0.8 kyrs BP (Fig. ~~3~~4a). Of these three Gd clusters, only the latter (0.8 kyrs BP) has the TnL (from 1.1 kyrs BP to 0.6 kyrs BP, Fig. ~~3~~4a) and the Gd significance points, reflecting a large~~big~~ environmental shift occurring at this time (1.1 kyrs BP – 0.6 kyrs BP), as can be inferred by the increase in the RoC at its maximum values (> 0.8, Fig. 3a).

~~However, when comparing with~~When taking into consideration only the 3.6 - 0.7 kyrs BP period, a cluster of TnL peaks is present from 3.2 to 3 kyrs BP, from 2.7 kyrs BP to 2.5 kyrs BP, from 1.2 to 1 kyrs BP, and a single point at 0.7 kyrs BP (Fig. ~~3~~4b). The ~~first one at~~ 3.2-3 kyrs BP event is coincident with the presence of a Gd clusters starting at 3.3 – 3 kyrs BP ~~kyrs BP~~ from the previous analysed period (Fig. ~~3~~4a), ~~while the second one is followed by a Gd clusters starting at 2.5 kyrs, that is coherent with the results of the previous analysis (Fig. 4). The 3.3-3 kyrs BP interval has both the TnL and Gd over the same~~

~~period. In addition, the RoC curves are flat, showing no distinctive trend and indicating no significant increase or decrease in the compositional change of the benthic foraminiferal community (Fig. 4). This suggests that the TE at 3.3-3 kyrs BP was probably caused by an environmental change that had no lasting impact on the benthic foraminiferal fauna.~~

~~The second period, from 2.7 to 2.5 kyrs BP, is characterized by TnL peaks followed by the Gd peaks (Fig. 4b), with the latter~~

300 ~~appearing in both analysis (Fig. 4).~~ Over the 3.6-2.7 kyrs BP period, both RoC curves show no distinctive trend, thus indicating no significant increase or decrease in the compositional change of the benthic foraminiferal community after the 3.3-3 kyrs BP event (Fig. 3). At 2.7-2.5 kyrs BP, TnL points are followed by Gd points (Fig. 3b), with the latter appearing in both analysis (Fig. 3). ~~Contrary to the previous TE at~~In contrast to the 3.3 – 3 kyrs B~~P period~~P, the presence of a visible downward trend of RoC curves after 2.5 kyrs BP suggest that this event~~TE~~ was caused by an environmental shift that had a long-term effect on

305 the fauna (Fig. 3b).

~~Another key difference between the two analysed periods is the presence of~~Afterwards, several TnL from 1.2 kyrs BP to 1 kyrs BP without being followed by Gd clusters are present, and a peak at 0.7 kyrs BP is reached (Fig. 3~~4~~b). Both the 1.2-1 kyrs BP and the 0.7 kyrs BP points are present over an upward trend (Fig. 3b).~~From the previous analysis a cluster of TnL was present from 1.1 kyrs BP to 0.6 kyrs BP (Fig. 4a). However, both TnL clusters are present over an upward trend (Fig. 4b) that~~

310 ~~can be related to an overall increase in the changes of community.~~ Th~~u~~is ~~can be caused by~~ a period that is characterized by a high degree of instability, probably reflecting a transitional period can be inferred (Mottl et al., 2021a). Hence, the period~~from~~ 1.2 ~~-to-~~1 kyrs BP is~~can be~~ connected to a different TE than the one at 0.7 kyrs BP, because of the segregation of the TnL clusters (Fig. 3~~4~~b). The ~~single 0.7 kyrs BP~~most recent TnL point (~~(~~Fig. 3~~4~~b) ~~can be connected to the~~is probably caused by a
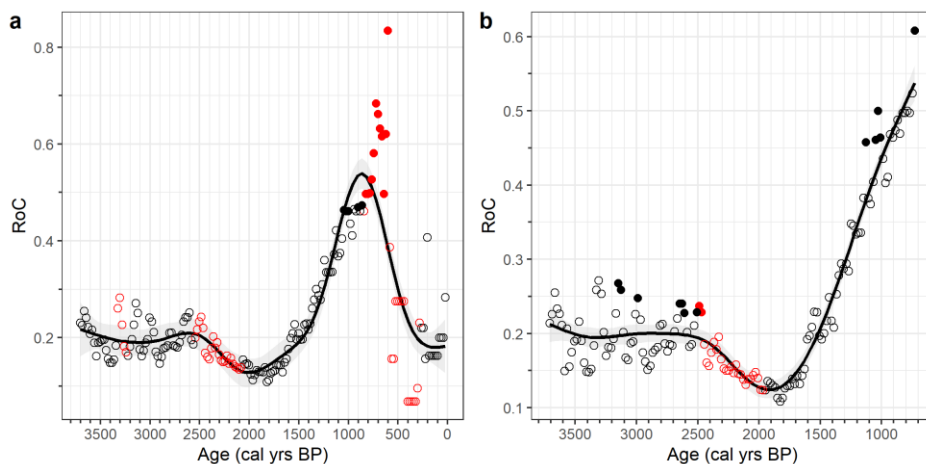
substantial environmental shifts happening at 0.7 kyrs BP. This is highlighted in the RoC computed throughout whole period,

315 reflected by the presence of both TnL and Gd peak, as well as by reaching the maximum RoC value at that time (Fig. 3~~4~~a).

Figure 4~~3~~. RoC analysis results on the benthic foraminiferal species. a) Results for the whole core; b) results of the analysis evaluated on the 3.6-0.7 kyrs BP. Red colors indicates the significance Gd points, while the black indicates the opposite. Filled circles indicates the significante TnL points. For further information the reader is referred to Fig. 3.

~~By these observations, we can define three distinct environmental shifts that influenced the long-term composition of the~~

320 ~~benthic foraminiferal assemblages: around 2.7 to 2.5 kyrs BP, from 1.2 to 1 kyrs BP and around 0.7 kyrs BP (Fig. 4). To better~~ ~~elucidate the connections between the TE and their effects on the benthic foraminiferal fauna, we compare the distribution of~~ ~~the most common species (relative abundance > 10%) throughout the record (Fig. 5).~~

The last 2 kyrs BP were previously investigated for the benthic association, and a succession of different environmental phases was hypothesized (Galli et al., 2023). Over this period, the benthic foraminiferal assemblages were indicative of a seasonal

325 sea-ice phase of the fjord (2-1.5 kyrs BP) followed by a transitional phase (1.5 – 0.7 kyrs BP) while the last 0.7 kyrs BP are indicative of a cold, and almost completely sea-ice covered fjord causing a sharp reduction in the sediment accumulation rate by an order of magnitude (Di Roberto et al., 2023, Tesi et al., 2020). Moreover, the transitional phase of the fjord culminated with a complete switch from a calcareous dominated fauna to an agglutinated dominated one at 1.1 kyrs BP (Galli et al., 2023, Fig. 4). This transition of the dominant test material, coeval with a regional reduction of 2°C over the Victoria Land Region

330 (Stenni et al., 2017). In this context, the RoC analysis agrees with this environmental evolution: lower values of the RoC over the 2-1.5 kyrs BP period are followed by a steeper increase of the compositional changes over the 1.5-0.7 kyrs BP (Fig. 3a). Over the increase instability of the community (increase in the RoC values), the presence of TnL at 1.2-1 kyrs BP, are coeval with the switch in the dominant component of the fauna (Fig 4): During the 2-1.5 kyrs BP interval, the fjord is transitioning from a seasonal sea-ice phase to a completely covered fjord after 1.1 kyrs BP (Galli et al., 2023). Thus, the RoC curve aligns

335 with the evolution of the sea-ice cover duration, with higher ecological instability increasing throughout the last 2 kyrs BP caused by the reduction of the ice-free period.

Following these interpretations, the presence of a difference in the average values of the RoC between 3.6-2.7 kyrs BP and 2.5-1.5 kyrs BP might be indicative of a switch of the state of the sea-ice cover during the summer, from a short ice-free period to a completely ice-free one at 2.7-2.5 kyrs BP. Moreover, the presence of TnL at 3.3-3 kyrs BP are indicative of this ecological

340 instability over the 3.6-2.7 kyrs BP period. On the other hand, lower RoC values and a clear downward trend over the 2.5-1.8 kyrs BP period, suggests a higher ecological stability associated with increasing ice-free conditions over the summer.
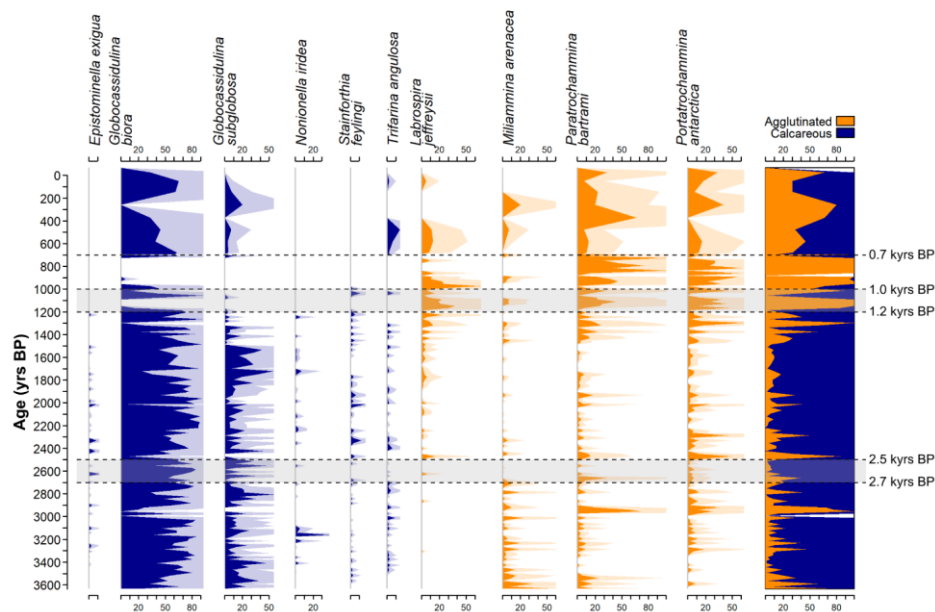
Figure 425. Benthic foraminifera relative abundances of the common species (> 10%) over the last 3.6 kyrs BP, divided as calcareous (blue) and agglutinated species (orange). Black dashed lines and grey area represent temporal locations of the turnover event as defined by the RoC analysis (see the text for further details). On the last panel on the right, the white areas represent barren samples. Shaded areas represent exaggerated silhouettes (x4) to enhance the visibility of the less common species. **All plots have the same scaling of the x-axis with one tick indicating a 10% relative abundance.**

The benthic foraminiferal species reflect this change in the system state. Throughout the From 3.6 to 1.5 kyrs BP period, the fauna is dominated by calcareous species such as *Globocassidulina biora* and *Globocassidulina. subglobosa* (> 50 % of the total assemblage, Fig. 54). These two common species Antarctic species have been found in Antartcic fjords and sub-ice shelf environments, and have been used as indicator species for high hydrodynamic activities of the bottom water, as well as high input of seasonal organic matter to the sea bottom (Bernhard, 1993; Harloff and Mackensen, 1997; Ishman and Szymcek, 2003; Kyrmanidou et al., 2018; Li et al., 2000; Majewski, 2023; Majewski et al., 2016, 2018; Melis et al., 2021; Sabbatini et al., 2004). In Admiralty Bay (King George Island, Antarctica) specimens belonging to the *Globocassidulina* group are the dominant species of fjord-like environment, even below 400 m water depth, with dead assemblage dominated by *G. biora* specimens (Majewski, 2005, 2010). Hence, the dominance of *G. biora* from the TR17-08 record implies the presence of a fjord-like environment. Agglutinated species such as *Paratrochammina bartrami* and *Portatrochammina antarctica* are also reported as a constituent of fjord-like environments, especially in the > 400 m water depth (Majewski, 2005, 2010). This is

also reflected in the TR17-08 records, with both species having low values of relative abundances (< 20%) with isolated peaks from 3.6 to 1.5 kyrs BP, paralleling the interpretation from ~~the~~ *G. biora* (Fig. ~~5~~4).

The RoC analysis highlighted an event at 3.3-3 kyrs BP that did not have a long-term effect on the faunal composition (Fig. 4b). This can be connected to the peak at 3.1 kyrs BP (> 20%) in the relative abundance of the opportunistic species *Nonionella iridea* that is ~~(Fig. 5). This species is known~~ known to prefer environment that are rich in organic matter and with steep oxygen gradients inside the sediments (Fig. ~~5~~4, Duffield et al., 2015). Thus, the abrupt increase of *N. iridea* could be connected to the presence of a substantial amount of organic matter arriving at the bottom, probably linked to an algal bloom in the surface layer. However, this event had no long-term effect on the benthic assemblage composition (Fig. ~~4~~3), probably reflecting an anomaly from the natural environment behaviour rather than a systematic change.

The TE occu ring~~identified~~ at 2.7-2.5 kyrs BP ~~can be connected~~is reflected by ~~to~~ the changes in the distribution of the calcareous species *Epistominella exigua, Stainforthia feylingi* and *Trifarina angulosa* along with the agglutinated species *Miliammina arenacea* and a sudden increase in the *Portatrochammina antarctica* (Fig. ~~5~~4).

The agglutinated miliolid species *M. arenacea* thrives in environments with high corrosive condition at the bottom and/or where cold and ~~saltier~~ salty water masses are present (Ishman and Szymcek, 2003; Li et al., 2000; Majewski et al., 2018; Murray, 1991). From 3.6 to 2.7 kyrs BP the relative abundance of this species is relatively constant through time (Fig. ~~5~~4). However, the period following the TE (2.5-1.5 kyrs BP) is characterized by the almost completely disappearance of this species (Fig. ~~5~~4). This change cannot be ascribed to an increase in the corrosive condition~~s for the carbonaceous fauna~~ as carbonate remains the dominant test material throughout the 3.6-1.5 kyrs BP interval (Fig. ~~5~~4). Hence, the disappearance of this species at 2.7 kyrs BP could be ascribed to a change in the water masses characteristics~~., probably to a switch from a colder to a warmer bottom water condition.~~

Even in low percentages, the presence of *E. exigua* in relative higher values during, and after, the TE can be indicative of the presence of warmer~~ ~~water mas~~s~~ses, as the mCDW, and the presence of phytodetritus~~phytodetritivourous~~ input from the top (Fig. ~~4~~5, Harloff & Mackensen, 1997; Ishman & Szymcek, 2003; Majewski et al., 2018; Sabbatini et al., 2004). The more continuous presence of high organic matter indicator~~of opportunistic~~ species such as *N. iridea* and *Stainforthia feyling*i, also suggest an increase flux of organic matter to the bottom~~in the phytodetritivourus input from the top~~ (Duffield et al., 2015; Knudsen et al., 2008; Seidenkrantz, 2013; Seidenstein et al., 2018).

~~In addition, The~~this overall increase in th~~ese species~~e ~~opportunistic species might~~can be ~~caused by~~ be attributed to the presence of more frequent and prolonged ice-free condition, having the effect of increasing the organic matter delivery to the bottom over the ice-free period, aligning with the RoC curve (Bart et al., 2018; Majewski and Anderson, 2009; Murray and Pudsey, 2004; Tesi et al., 2020). This is further supported by the sharp increase of *Portatrochammina antarctica*, an agglutinated species sensitive to increases in the primary production (Majewski et al., 2020).

Moreover, species as *Trifarina angulosa* has been used as an indicator species of high energy environment at the bottom, reflecting the presence of bottom water circulation (Ishman and Szymcek, 2003; Melis and Salvi, 2009). Despite being in low

percentages, the presence is homogeneous throughout the 3.6-1.5 kyrs BP period, except ~~from~~ the 2.7-2.5 kyrs BP interval (Fig. ~~5~~4), probably reflecting a decrease in the strength of the circulation over this time.

~~Hence, over the 3.6 – 1.5 kyrs BP interval, the TE at 2.7-2.5 kyrs BP might reflect a period of major environmental shift. From 3.6 to 2.7 kyrs BP, the fjord is characterized by cold bottom water conditions, a bottom water circulation and less primary productivity. At 2.7-2.5 kyrs BP the transition happens and after the TE, from 2.5 to 1.5 kyrs BP, the fjord is characterized by intrusions of a warm water mass and an increase in primary productivity and organic matter flux at the sea bottom (Fig. 5).~~

~~The following TE, at 1.2 -1 kyrs BP, can be connected to the abrupt increase of the agglutinated forms respect to the calcareous one (Fig. 5). More specifically, significant increases of the species *L. jeffreysii, P. bartrami* and *P. antarctica* are present, concomitantly with an abrupt decrease in the *G. biora* relative abundance and the almost complete disappearance of *G. subglobosa* (Fig. 5). This also hints to an overall decrease in the circulation strength as testify by the high relative abundances of both *P. bartrami* and *P. antarctica,* characterized by tests with high mechanical fragility, by the increases in the *M. arenacea* relative abundance starting at 1.5 kyrs BP and by the absence of *T. angulosa* (Capotondi et al., 2018, 2020). This high dissolution condition persisted until 0.7 kyrs BP, as suggested by the agglutinated forms being the dominant benthic foraminiferal fauna (Fig. 5).~~

~~Lastly, at 0.7 kyrs BP another TE took place, but it might be related to the significant reduction in the sedimentation rate (Fig. 2). In addition, the presence of both the calcareous and agglutinated forms in similar percentages makes the interpretation difficult without a proper environmental context (Fig. 5).~~

Hence, over the 3.6 – 1.5 kyrs BP interval, from 3.6 to 2.7 kyrs BP, the fjord is characterized by cold and salty bottom water conditions, a bottom water circulation and less primary productivity, with higher RoC values indicating a less ice-free condition over the summer season. At 2.7-2.5 kyrs BP the transition occurs, with the diseappearance of *T. angulosa* suggesting a shutting down of the bottom water circulation. From 2.5 to 1.5 kyrs BP, the benthic fauna suggests more intrusions of mCDW, an increase in both primary productivity and organic matter flux to the sea floor (Fig. 4). The presence of the RoC values over this period suggests the presence of a prolonged period of ice-free conditions over summer.

3.2 Environmental ~~**conditions over the last 3.6 kyrs BP**~~**transition at 2.7-2.5 kyrs BP**

To have a ~~more~~ comprehensive view of the environmental ~~evolution~~ transition ~~of the~~ that characterized Edisto Inlet ~~over~~around 2.7-2.5 kyrs BP~~the last 3.6 kyrs BP, we compared~~ the RoC curves and the benthic assemblages (Fig. 4) were compared with the ~~micropaleontological and~~ geochemical proxies derived from the TR17-08 sediment core, as well as previously published records from the same core and others derived from nearby marine sediments cores (Fig. 1c, HLF17-01 and Bay05-20c) (Galli et al., 2023, 2024; Mezgec et al., 2017; Tesi et al., 2020). A summary of the intepretations is reported in Table 1.

~~As said in section 3.1, RoC values are indicative of the compositional changes that are inferring on the benthic foraminiferal community. Since the depositional settings of Edisto Inlet is mostly governed by the seasonal cycle of freezing-thawing of the sea-ice cover, the RoC values can also be connected to the environmental stability of the summer season, when most of the sediment accumulations happens (Di Roberto et al., 2023; Tesi et al., 2020). Then, higher RoC values should reflect a period~~

Formattato: Tabulazioni: 5,25 cm, Allineato a sinistra

425 in which the summer is not long enough for a stable community to form. On the other hand, lower values should reflect periods in which the community is changing at a slower pace, thus becoming stable.

In addition to the geochemical proxy described in the section 2.4, other micropaleontological proxy were analysed. We evaluated the accumulation rates of the benthic foraminifera (BFAR) and the planktic foraminifera (PFAR), that have been extensively used as a tracker for the flux of organic matter at the seafloor and as a proxy for primary productivity, respectively

430 (Herguera and Berger, 1991; Kyrmanidou et al., 2018; Majewski and Anderson, 2009; Peck et al., 2015). Furthermore, the probability of occurrence of *Ophionotus victoriae* (P(O)), a common Antarctic brittle star species, was used as a proxy for interannually consistent sea-ice cycle, with higher values reflecting the latter (Fig. 5a, Galli et al., 2024; Grange et al., 2004). We also compared the $IPSO_{25}$ derived from the HLF17-01 that reflects prolonged ice-free period summer over Edisto Inlet during the last 2.6 kyrs BP (Belt et al., 2016; Tesi et al., 2020), and the relative abundances of the diatom *Fragilariopsis curta*

435 derived from the Bay05-20, that can be used to infer changes in the pack-ice and primary productivity (Mezgec et al., 2017). The summary of the environmental evolution of the Edisto Inlet over the last 3.6 kyrs BP is reported in Table 1.

ha formattato: Inglese (Regno Unito)

Figure 6~~5~~. Paleoenvironmental ~~reconstruction~~ evolution from ~~of the last~~ 3.6 kyrs BP to 1.2 kyrs BP in Edisto Inlet. Different background ~~colors~~colours ~~correspond to different environmental phases~~are used to highlight the transition from a multi-year sea-ice environment to a seasonal sea-ice one. Vertical black dotted lines ~~and yellow areas represent~~ are indicative of the significant Turnover Events (TEs) as defined in the section 3.1. a) Rate-of-Change (RoC) results (points) and fitted GAM models (line) throughout the core (in black) and for the 0.7-3.6 kyrs BP period (~~in purple~~in light blue). The red line indicates the *Ophionotus victoriae* presence modelled as the probability of occurrence (P(O), from Galli et al., 2024). Note the inverted scale for the P(O) to highlight the similarities with the RoC curves. The names highlight the difference benthic foraminiferal species disucsses in section 3.1 with + symbol indicating more presence and – symbol indicating less presence ~~; b) Probability of occurrence of Ophionotus victoriae (P(O)) from Galli et al. (2024) (Orange area); c~~c) ~~Benthic Foraminifera Accumulation Rate (BFAR, black area); d) Planktic Foraminifera Accumulation Rate (PFAR, green area); e) Ice Rafted Debris flux (IRD, blue area); b~~b) logarithm in base 10 of the ratio ~~Br/Ti~~Zr/Rb (~~brown~~gray dots referred to raw data, ~~black~~brown line represent the fitted LOESS); c~~g~~) Primary productivity indicators: Ca/Ti (green~~) and h~~) ~~Zr/Rb~~Br/Ti (~~black~~purple); d) Ice Rafted Debris flux (IRD, blue, from Galli et al., 2024). e) Benthic Foraminifera Accumulation Rate (BFAR, brown) and Planktic Foraminifera Accumulation Rate (PFAR, dark blue, from Galli et al., 2024). The logarithm in base 10 was applied to enhance the ~~enhance~~ variability of the fluxes values; f) Fragilariopsis curta relative abundance from the core BAY05-20.g~~i~~) IPSO$_{25}$ values in logarithm in base 10 from the HLF17-01 with blue and red triangle indicating different summer sea-ice cover~~: in red is indicated the ice-free summer, in blue the presence of summer sea-ice cover (Tesi et al., 2020); j) Fragilariopsis curta relative abundance from the core BAY05-20. The red dotted line indicates the 60% relative abundance thresholds. Above 60% can be regarded as substantially prolonged ice-cover period (Allen et al., 2021); k) magnified window of the 2.6-2.5 period (see section 3.2.2) for further information.~~

3.2.1 From 3.6 kyrs BP to 3.5 kyrs BP

~~Although there are only a few data points covering this period, some interpretations of the environmental conditions can still be made (Fig. 6).~~

~~Near zero values of the BFAR and PFAR suggests a low flux of organic matter at the bottom, as well as low primary productivity (Fig. 6c-d). However, this is the only period where there is a discrepancy between the Br/Ti, having relatively high values, and the Ca/Ti, showing a decreasing trend (Fig. 6f-g). A period of high carbonate dissolution could explain this discrepancy between the geochemical proxies and the foraminiferal contents, especially for the PFAR since it is derived from the only planktic foraminifera present in the core. This is also supported by the high relative abundance (> 20%) of *M. arenacea*, reflecting higher dissolution conditions (Fig. 5).~~

~~However, the few points of the records make it difficult to assess the environmental conditions inferring in the Edisto Inlet over this period.~~

~~3.2.2 From 3.5 kyrs BP to 2.5 kyrs BP~~

~~The RoC curves over this period are characterized by having a constant trend and a high variability (Fig. 6a). In addition, the presence of a TE at 3.3-3.1 kyrs BP which is not connected to a long-term change (Fig. 4), might suggests a period with highly variable environmental conditions over the summer seasons. The benthic foraminiferal fauna hinted to the presence of bottom currents, cold bottom water conditions, and low productivity (Fig. 5). While the presence of bottom currents can also be inferred by the constant values of the Zr/Rb ratio (Fig. 6h), the other proxies behave differently.~~

~~Galli et al. (2024), associated the high values of BFAR, PFAR and IRD to an increase in the organic matter flux to the sea floor with the presence of explosive primary productivity episodes (Fig. 6c-e). The TE at 3.3-3.1 kyrs BP which is connected~~

the peak of the opportunistic *Nonionella iridea* strengthen this hypothesis (Fig. 5). However, both Br/Ti and Ca/Ti ratios are increasing throughout, hinting to a gradual increase in the primary productivity (Fig. 6f-g).

The presence of prolonged periods with multiyear landfast sea-ice could explain these apparent discrepancies. The present-day setting of Edisto Inlet is mainly controlled by the presence of seasonal landfast ice (Battaglia et al., 2024; Tesi et al., 2020). Landfast ice is prone for being multi-year and can shows high nutrient concentrations, since they can be stored and accumulate on the basal portion of the sea-ice for multiple consecutive years. This could lead to an increase in the sea-ice associated diatoms, hence resulting in abrupt increase of the primary productivity upon the first break-up (the so called "high nutrient high chlorophyll paradox"; Fraser et al., 2023; Wongpan et al., 2024). Thus, while the surface productivity can be high in short-time frame due to the presence of algal blooms, explaining the peaks of the BFAR and the PFAR values, it also might not have any effect in longer time frame as shown in the Br/Ti and Ca/Ti ratios because of the prolonged presence of the landfast ice cover (Fig. 6f-g). The low *Fragilariopsis curta* relative abundances in the marine sediment core Bay05-20 also support this interpretation, since without a thawing season, this sea-ice indicator diatom cannot thrive, hence relatively low values (Fig. 6j) (Leventer et al., 1993; Mezgec et al., 2017; Waters et al., 2000).

The increase in the overall primary productivity over the 3.5-2.5 kyrs BP period as indicated by Br/Ti and Ca/Ti ratios, can be associated to the positive trend of presence of *Ophionotus victoriae* (Fig. 6b). The probability of occurrence of this brittle star (P(O)) has been connected to interannually stable sea-ice cycle. Hence, P(O) along with Br/Ti and Ca/Ti, might be used to track the increase in the break-up events frequency, probably reflecting milder conditions towards the end of this phase.

At the end of this climatic phase, over the 2.7-2.5 kyrs BP period, a TE in the benthic foraminifera is present (Fig. 6).

In section 3.1, we showed that this TE can be connected to a transition between a cold bottom water, low productivity setting to a warm water mass, high productivity setting (Fig. 5).

This significant switch in the benthic foraminiferal composition happens in conjunction with a sudden reduction of the Zr/Rb values (Fig. 6k), and a peak in both the Br/Ti and Ca/Ti ratios (Fig. 6f-h). The decrease in the Zr/Rb can be indicative of a general decrease in the circulation strength in the fjord (Wu et al., 2020). In addition, this proxy has stable values over the 2.6-2.5 kyrs BP and progressively increases from 2.5 kyrs BP onwards, probably reflecting a period in which the currents strength was low (Fig. 6k). This is also consistent with the absence of *Trifarina angulosa* over this period (Fig. 5).

The spikes of the Ca/Ti and the Br/Ti suggest high primary productivity (Ziegler et al., 2008). The increase in the primary productivity along with the change in the circulation strength, may be related to an increase of the meltwater derived from the glacier, or glacial run-off. Glacial run-off in fjords have the effects of enhancing the mixing of the water column, delivering nutrient and could positively affect the thermoaline circulation (Howe et al., 2010; Pan et al., 2020).

Moreover, an increase in the glacier run off could also be consistent with this trend of reducing multi-year sea-ice events over this period, culminating with a conspicuous meltwater flux that acted as a stress for the benthic foraminiferal community, reducing the circulation strength and enhancing the organic matter flux to the sea bottom and the primary productivity (Forsch et al., 2021; Howe et al., 2010; Korsun et al., 2023; Pan et al., 2020).

3.2.3 From 2.5 kyrs BP to 2 kyrs BP

After the 2.7-2.5 kyrs BP event (Fig. 6k), the benthic foraminiferal RoC curve shows a downward trend, probably reflecting increasing stability of the summer season, consistent with the steeper increase in P(O) (Fig. 6a-b) (Galli et al., 2024). The Zr/Rb ratio is increasing from 2.5 to 2 kyrs BP (Fig. 6h), suggesting a slow restoration of the circulation strength of the fjord.

The BFAR and the PFAR values diminishes over this period, while simultaneously becoming more stable, with frequently less peaks in comparison to the previous phase (Fig. 6c-d). Moreover, the relatively low content of IRD can be connected to the presence of more prolonged ice-free conditions over the summer season (Fig. 6e) (Christ et al., 2015; Galli et al., 2024; Peck et al., 2015). Supporting this interpretation of an increasing prolonged sea ice-free condition over the austral summer, the Br/Ti and Ca/Ti shows a downward trend, that may reflect an oligotrophisation of upper water column derived from prolonged period of open sea condition (Fig. 6f-g). In addition, from 2.5-2.3 kyrs BP the IPSO$_{25}$ have lower values indicating the presence of seasonal ice-free condition in the fjord (Fig. 6i). However, from 2.3 to 2 kyrs BP, there is an increasing trend of these values, that can be connected to a later thawing of the seasonal sea-ice cover.

Over this period, the benthic foraminifera fauna suggested the presence of intrusions of warm water masses as well as an environment with a high organic matter content which is consistent with the other proxies (Fig. 5).

Fragilariopsis curta relative abundance in core Bay05-20 also hints to an increase in the sea-ice duration, since its relative abundance almost reach the 60% threshold that can be connected to prolonged winter sea-ice presence (Allen and Weich, 2022; Leventer et al., 1993; Waters et al., 2000) (Fig. 6j).

In conclusion, this phase can be connected to a period where the fjord is experiencing a switch from a multi-year sea-ice to a seasonal sea-ice dominated environment, that is connected through the 2.7-2.5 kyrs BP event. However, seasonality is not stable from year to year, probably reflecting the presence of episodic multi-year sea-ice events.

3.2.4 From 2 kyrs BP to 1.55 kyrs BP

Over this period, the RoC curves values are the lowest, while the P(O) is the highest, hinting to the most stable environmental phase in regards of the seasonal sea-ice cycle (Fig. 6a-b) (Galli et al., 2024). This period was previously identified as the Ophiuroid Optimum, a period in which the fjord is experiencing interannually stable conditions of freezing and thawing of the sea-ice cover, reflecting prolonged free-ice period over the austral summer period (Galli et al., 2024). This period was identified by noticing that the maximum P(O) happens simultaneously with the lowest average values of the IPSO$_{25}$ (Fig. 6i) (Tesi et al., 2020). The presence of a prolonged period of summer sea-ice free conditions, can also be inferred by the other proxies. The low but stable values of BFAR and PFAR can be connected to a lower variability of the nutrient input, while the IRD are characterized by their lowest values indicating the presence of a seasonal sea-ice cover that is thawing during the summer season (Fig. 6e) (Christ et al., 2015; Galli et al., 2023, 2024). A further indication of the stability of the seasonal sea-ice cycle is suggested by the downward trend of the *F. curta* that can be interpreted as a prolonged ice-free season (Mezgec et al., 2017).

Moreover, the Br/Ti and Ca/Ti ratios are increasing throughout this environmental phase, probably reflecting an increase in the nutrient input, while the downward trend of the Zr/Rb ratio suggests a gradual decrease in the circulation strength (Fig. 6f-h). This changing can also be ascribed to an increase in the prolonged ice-free period. A strengthening of the glacial runoff provides nutrient through sediment input over the ablation season while reducing the circulation strength by increasing the meltwater content of the water column (Howe et al., 2010; Pan et al., 2020).

3.2.5 From 1.55 to 0.7 kyrs BP

This phase is characterized by the steady increase of the RoC values, culminating at 0.7 kyrs BP, and by the reduction of P(O) which reaches 0, reflecting the onset of environmental instability that is culminating at the end of the phase (Fig. 6a-b).

In a previous study, it was suggested that an increase in the stratification of the water column led to oxygen poor and corrosive conditions on the bottom, probably as consequence of a conspicuous freshwater input from retreating glaciers (Galli et al., 2023). This meltwater pulse event might have had the long-term effect of excluding the fjord from the regional circulation, reducing the nutrient supply and increasing the sea-ice cover duration (Carvalho et al., 2016; Galli et al., 2023; Pauling et al., 2017).

The initial abrupt decrease in the Zr/Rb values at the beginning of the phase can be indicative of reduction of the circulation, consistent with the interpretation (Fig. 6h).

The fauna become dominated by agglutinated forms, suggesting an increase in the corrosive conditions probably due to the increase in the residence time of the water masses (Fig. 5). Around 1.5 kyrs BP there is a marked reduction of *Globocassidulina subglobosa* while the other agglutinated species starts to increase (Fig. 5). The complete disappearance of the calcareous fauna starts gradually around 1.5 kyrs BP, culminates around the TE, and lasts until 0.7 kyrs BP (Fig. 5).

A drop in the primary productivity can be inferred by the decreasing values of both the BFAR and PFAR, reaching zero at 1.2 kyrs BP (Fig. 6c-d), while the Br/Ti and Ca/Ti are also decreasing until 1.1 kyrs BP (Fig. 6f-g). Interestingly, this coincides with the TE in the benthic foraminiferal community located at 1.2 – 1 kyrs BP, and the sudden increase in the IRD content from the same period (Fig. 6h).

In addition, the TE happens in concomitance of a sudden increase in the *F. curta* content > 60%, as well as high IPSO$_{25}$ concentrations, reflects prolonged sea-ice cover conditions (Fig. 6i-j).

Moreover, in Galli et al., (2023), this phase corresponds to a transitional phase of fjord from a seasonal to a non-seasonal dynamic, from open to close in respect of the circulation pattern. This is in accordance with the results shown in this study.

3.2.6 From 0.7 kyrs BP to recent

Over this period, as previously shown by other studies in the region, there is a presence of an abrupt shift in the sedimentation rate of about one order of magnitude (Di Roberto et al., 2023; Tesi et al., 2020). The cause of this shift has been attributed to the presence of perennial sea-ice cover, or experience very short or restricted opening (Galli et al., 2023; Tesi et al., 2020).

The extremely low values of BFAR and PFAR can be the consequence of the onset of harsher environmental conditions, as also suggested by the Br/Ti and Ca/Ti (Fig. 6c-d; Fig.6f-g). This can also be deducted by the absence of *O. victoriae* (Fig. 6b).

575 The other nearby cores shows a similar behaviour: the presence of above threshold values of the IPSO$_{25}$ with the presence of an > 60% of *F.curta*, can be connected to the increase in the prolonged sea-ice conditions (Fig. 6i-j).

Further speculation is complicated due to the drop of sedimentation rate that can hide short-term changes over this period.

Over the 3.6 – 2.7 kyrs BP, higher RoC values occur along with the low probability of occurrence of the ophiuroid *Ophionotus victoriae* (P(O), Fig. 5a). Lower values of the P(O) can be associated with unstable seasonal sea-ice conditions due to the

580 dependency of this organism to stable interannual conditions (Fig. 5a, Galli et al., 2024). The benthic foraminiferal assemblage suggests the presence of bottom currents, cold and salty bottom water conditions and low productivity (Fig. 5a). Presence of bottom currents are also suggested by stable values of the Zr/Rb ratio (Fig. 5b), while the low values of both the Ca/Ti and Br/Ti are indicative of a low primary productivity (Fig. 5c) However, in Galli et al. (2024) the high variability of the BFAR and PFAR have been associated to an increase in the organic matter flux to the sea floor with the presence of abrupt increases

585 of primary productivity (Fig. 5d, e), also suggested by the peak of *Nonionella iridea* at 3.1 kyrs BP (Fig. 4). The presence of prolonged periods with multiyear landfast sea-ice could explain these apparent discrepancies between the geochemical and micropaleontological proxy. The present-day setting of Edisto Inlet is mainly controlled by the presence of seasonal landfast sea-ice (Battaglia et al., 2024; Tesi et al., 2020). Landfast sea-ice is prone to become multi-year and can show high nutrient concentrations, since they can be stored and accumulate on the basal portion of the sea-ice for multiple consecutive years. This

590 could lead to an increase in the sea-ice associated diatoms, hence resulting in abrupt increase of the organic matter flux to the bottom upon first break-up (the so called "high nutrient high chlorophyll paradox"; Fraser et al., 2023; Wongpan et al., 2024). Thus, while the surface productivity can be high in short-time frame due to the presence of algal blooms, as indicated by the BFAR and the PFAR values, this might not have any effect in longer time frame as shown in the Br/Ti and Ca/Ti ratios because of the prolonged presence of the ice cover (Fig. 5c). In addition, low percentages of *Fragilariopsis curta* from the nearby

595 Bay05-20 sediment core also support this interpretation, since without the presence of a seasonal sea-ice regime, this diatom cannot thrive, explaining the relatively low values in respect to the subsequent phase (Fig. 5f) (Leventer et al., 1993; Mezgec et al., 2017; Waters et al., 2000).

At 2.7-2.5 kyrs BP the TE in the benthic foraminifera highlights the transition from a cold and salty bottom water and low productivity setting to a state in which intrusion of mCDW along with a high primary productivity are present, as suggested

600 by the presence in higher abundance of *E. exigua* and the absence of *M. arenacea* (Fig. 5a). In addition, the absence of *T. angulosa* suggests the absence of a bottom current circulation over this short time interval (Fig. 5a).

These changes in the benthic foraminiferal composition occur in conjunction with a sudden reduction of the Zr/Rb values (Fig. 5b), and a peak in both the Br/Ti and Ca/Ti ratios, aligning with the benthic foraminifera interpretation (Fig. 5c).

The increase in the primary productivity along with the change in the circulation strength, might be related to an increase of

605 the meltwater derived from the marine terminating glaciers. Glacial meltwaters in enclosed basin have the effects of enhancing the mixing of the water column, increasing the nutrient content while strengthening the thermohaline circulation (Howe et al.,

2010; Pan et al., 2020). However, if the increase in the meltwater content exceeds a certain value, the presence of a high content of freshwater can reduce and even shut down the thermohaline circulation (Pan et al., 2020).

After the 2.7-2.5 kyrs BP event, the benthic foraminiferal RoC reaches the lowest values reflecting an increasing stability of

610 the summer season (Fig. 5a). This aligns with the macrofaunal response: the P(O) increases to its maximum values, suggesting a stable interannual seasonal sea-ice cycle (Galli et al., 2024). The Zr/Rb ratio is increasing from 2.5 to 1.8 kyrs kyrs BP (Fig. 5b), suggesting a slow restoration of the thermohaline circulation inside the fjord in accordance with the frequent presence of *T. angulosa* (Fig. 4). Both the Ca/Ti and Br/Ti identifies a period characterized by a higher average values in respect to the 3.6-2.7 kyrs BP, suggesting an increase in the primary productivity as well as increase in the organic matter flux to the bottom,

615 consistent with more frequent presence of *N. iridea* and *S .feylingi*, as well as an increase in the *Epistominella exigua* content (Fig. 5a). This species became more frequent over the 2.5-1.5 kyrs BP interval suggesting an increase in the mCDW intrusion inside the inlet (Fig. 4). Intrusion of this warm and nutrient rich water mass can cause the increase in primary productivity as well as a stabilizing the summer condition, promoting prolonged ice-free austral summer (Dinniman et al., 2011; Dale et al., 2017). This aligns with the BFAR and the PFAR record that suggest a more stable input of organic matter in respect to the

620 previous phase (Fig. 5d, Galli et al., 2024). Moreover, the relatively low content of IRD is indicative of prolonged ice-free conditions over the summer season, implying the presence of a seasonal sea-ice cover (Fig. 5d) (Christ et al., 2015; Galli et al., 2024; Peck et al., 2015). In addition, the *Fragilariopsis curta* in core Bay05-20 increases its relative abundances over this period, strengthening the hypothesis of a seasonal sea-ice regime (Allen and Weich, 2022; Leventer et al., 1993; Waters et al., 2000) (Fig. 5f).

625 Moreover, the period from 2 to 1.5 kyrs BP has been proposed to be the most "stable" in respect to the seasonal sea-ice phase of the fjord due to high P(O) and lowest IPSO$_{25}$ values (Fig. 5a-g, Galli et al., 2024). This is supported by the presence of lowest values of the RoC, indicating the presence of prolonged ice-free period promoting the benthic community stability.

Interval (yrs BP)	Proxy	Species Presence	Interpretation
3.6-3.5	†IRD; Zr/Rb; Br/Ti; *F. curta.* ↓ BFAR; PFAR; Ca/Ti.		High carbonate dissolution condition.
5-2.75	↑ IRD; BFAR; PFAR; Zr/Rb; P(O). - RoC. ↓ *F. curta*; Ca/Ti; Br/Ti.	↑ *M .arenacea* and *T. angulosa*. ↓ *E. exigua, N. iridea, S. feylingi.*	Cold and salty bottom; sea-ice cover; Decrease of this events at the 2.7-2.5 TE connected to an increase in glacier run-off.

75-2.5	↑ P(O); Zr/Rb. Br/Ti; Ca/Ti. RoC ↓RoC; IRD; BFAR; PFAR; Br/Ti; Ca/Ti.	↑ *E.exigua* ↓ *M. areancea* and *T. angulosa*	Warm water mass intrusion; onset of a seasonal sea-ice co... not stable with presence of multi-year sea-ice. Transitional event related to the interaction between the
5-1.555	↑ P(O); Br/Ti; Ca/Ti. - IRD; BFAR; PFAR. ↓ RoC; Zr/Rb; IPSO$_{25}$.	↑ *E.exigua*; *N. iridea*, *S.feylingi* and *T. angulosa* ↓ *M. areancea*	Stable phase: interannually stableSeasonal sea- Optimum).phase mCDW and high primary productivity.
55-0.7	↑ RoC; IRD; Zr/Rb; *F. curta*. ↓ BFAR; PFAR; Br/Ti; Ca/Ti; P(O).		Transitional phase: Meltwater pulse at the beginning of this phase; cooling starts at 1.2 kyrs BP.
- recent	↓ Sedimentation rate.		Cool phase: prolo... cover or very short openings during the summer.

Table 1. Major climatic phases in the Edisto Inlet over the last 3.6 kyrs BP. Associated with the climatic phase in kyrs BP, a qualitative description of the TR17-08 proxy behaviour (↑= relatively high, ↓= relatively low, - no change) and the schematic environmental phase description. For further detail the readers are referred to the section 3.2 of this manuscript.

3.3 Edisto Inlet as a sentinel for the ocean dynamics in the Ross Sea over the Late Holocene

Here we focus on the environmental evolution from 3.5 to 1.5 kyrs BP, especially on the environmental transition that happens in the Edisto Inlet around 2.7-2.5 kyrs BP, as identified from the TE of the benthic foraminifera, the low values of the Zr/Rb and the peaks in both the Br/Ti and Ca/Ti ratios (Fig. 5).

The event at 2.7-2.5 kyrs BP can be connected to a shift from a multi-year sea-ice dominated environment to a more open and seasonal sea-ice environment (Table 2). The benthic foraminiferal assemblage compositional changes also hint to a switch from a colder bottom water condition to a warmer one, probably the mCDW (Fig. 5).
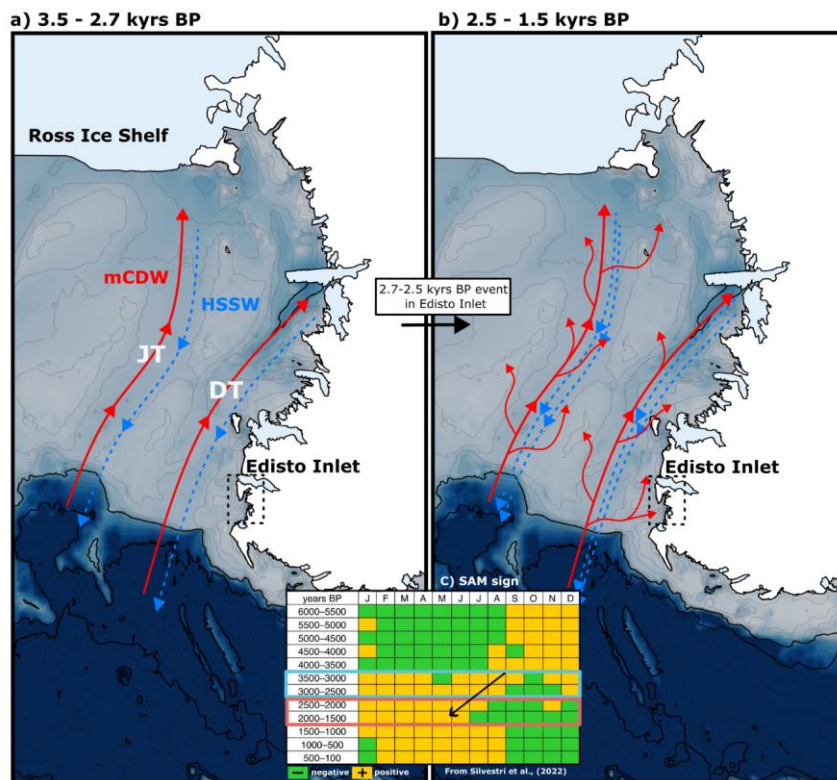
Figure ~~7~~6. Conceptual regional model of the oceanographic changes in the Ross Sea over the last 3.6 kyrs BP as identified in Edisto
Inlet (black dotted square). Red arrows indicate the schematic flows of the superficial mCDW intrusions. Blue arrows indicate the
flow of the deeper HSSW. DT= Drygalsky Through, JT = Joides Through. a) oceanographical situation from 3.5 to 2.6 kyrs BP; b)
oceanographic circulation from 2.5 to 1.5 kyrs BP; c) Southern Annular Mode values (positive in orange, negative in green) divided
by month. The period covered from the panel a) is highlighted by the blue square on the years BP column. The panel b) is highlighted
by the red square on the years BP column. Adapted from Silvestri et al. (2022).

Over the Victoria Land Coast, and in general over the Ross Sea, ~~different studies with~~ different proxies refer~~s~~ to a similar period as the enviromental transition occurring in Edisto Inlet regarding the sea-ice conditions. ~~for an environmental transition.~~ Hall et al. (2023) studying the distribution of the southern elephant seals (*Mirounga leonina*) remains over the Mid and Late Holocene inferred an increase in the open water conditions, as well as a reduction in the sea-ice presence, from 2.3 to 1.8 kyrs BP. They ascribed this ecological dynamic to an increase in the modified ~~Circumpolar Deep Water (mCDW)~~mCDW intrusion over the Victoria Land, having a strong negative effect on local marine terminating glacier (Hall et al., 2006, 2023).

Another ~~proxy~~ tracer ~~that has been used for the reconstruction~~ of the mCDW intrusion over the Ross Sea is the presence of the Adelie penguin (*Pygoscelis adeliae*) colonies (Hall et al., 2023; Xu et al., 2021). Adelie penguins occupy a different ecological niche than elephant seals despite relying on the presence of a free-ice zone to feed (Emslie et al., 2003, 2018; Hall et al., 2006). Since Penguins ~~relies~~rely on the presence of a consolidated ice platform to breed, while the elephant seals do no~~t, due to the increased nukber of penguin colonies t~~. ~~By comparing the presence of an increased number of colonies of penguins~~ ("Penguin Optimum", 4.6 -2.8 kyrs) followed by an increase in~~and~~ of southern elephant seals colonies ("Southern elephant seals optimum", 2.3-1.8 kyrs BP), Hall et al. (2023) inferred that over the 5-2.7 kyrs BP the Victoria Land region was a landfast ice dominated environment, while, from 2.5 kyrs BP to 0.5 kyrs BP a period of warmer-than- present climate ~~onset~~ that may be related to a strengthening of the mCDW intrusion.

The~~is~~ switch in the sea-ice conditions over the Victoria Land region ~~this region~~ is coeval with ~~o~~ the TE occurring ~~on the benthic foraminifera community ur event located~~ at 2.7-2.5 kyrs BP (Fig. 6~~5~~), ~~that could~~ This local transition might be linked to this regional response of ~~an~~the increase intrusion of mCDW over the western coast of the Ross Sea ~~Victoria Land Coast~~ (Fig. 7~~6~~). ~~Despite not having direct evidence of recent mCDW intrusion in Edisto Inlet, an overall increase of this water mass inside the fjord can be connected to our environmental shifts.~~ An ~~increase~~ addition of ~~in~~ the overall content of mCDW ~~can~~could 1) ~~increase~~ sustain the stability of the free-ice period; 2) increase the glacial input derived from the melting of the marine terminating glacier and 3) ~~increases~~ enhance the primary productivity, due to the high nutrient concentration that this water mass has (Arrigo and van Dijken, 2004; Dale et al., 2017; Dinniman et al., 2011; Emslie et al., 2003; Hall et al., 2006; Mathiot et al., 2012; Orsi and Wiederwohl, 2009; Smith et al., 2012; Smith and Gordon, 1997; Wang et al., 2023; Xu et al., 2021). Over the transition period, the intensification of glacier run-off would have promoted the thawing of the marine terminating glaciers and increasing the meltwater content. This has the effect of reducing the circulation inside the inlet, thus implying a stronger influence of the mCDW over the study area. In addition,

The presence of mCDW inside the inlet is ~~also~~ reasonable due to the ~~water mass properties~~bathymetric distribution that this water mass over the Ross Sea region. The mCDW is generally found at depth of around 200-400 m ~~and~~, within the Drygalski ~~through~~through, this water mass ~~and flows~~ flows ~~southward~~, consistent with the~~geo~~morphological features of ~~the~~the Edisto Inlet (Castagno et al., 2017; Orsi and Wiederwohl, 2009; Smith Jr. et al., 2014; Wang et al., 2023; Zhang et al., 2024).

Since this should be a regional resoponse, a re~~Another~~ key element is the presence of a relation between ~~more~~ the upwelling of mCDW ~~intrusion~~ onto the contintental shelf and the positive phases of the Southern Annular Mode (SAM, fig. 6~~7~~c). The SAM is defined as a latitudinal gradient of sea-level pressure between mid and high latitude (Fogt and Marshall, 2020; Marshall, 2003). Positive phases of this atmospheric modes are associated with the strengthening and the poleward movement of the westerlies, that~~,~~ in turns~~,~~ increase~~ss~~ the upwelling of the CDW onto the continental shelf and~~, increasing~~ the production of the HSSW and enhances the efficiency of the polynya ~~and, lastly, inducing a strengthening of the katabatic wind that ultimately controls the polynya ice-free area~~ (Campbell et al., 2019; Gordon et al., 2007; Zhang et al., 2024). ~~In a simulation using state-of-the-art models, Silvestri et al. (2022), showed an increase in the positive phases of the SAM over the austral summer that is consistent with the seasonal sea-ice phase detected in Edisto (Fig. 7c). A shift from more prolonged~~

685 and positive SAM condition over the summer period is present throughout 2.5-1.5 kyrs BP, that can be linked to the presence of this mCDW intrusions. . In a simulation using state-of-the-art models, Silvestri et al. (2022), showed an increase in the positive phases of the SAM in the austral summer over the 2.5-1.5 kyrs BP (Fig. 6c) that is consistent with the transition that characterized Edisto Inlet sea-ice regime (Fig. 6c).

A shift from more prolonged and positive SAM condition over the summer period is present throughout the 2.5-1.5 kyrs BP

690 period, causing more prominent mCDW intrusions over the Victoria Land Coast, ultimately causing more intrusion of this water mass inside the inlet, sustaining the ice-free season (Fig 6).

This is also consistent with the study Mezgec et al., (2017) that compared marine and ice core records. In their study, increases in the of the polynya efficiency along with an increase in the katabatic wind regimes was hypothesized starting around 2.5 kyrs BP, which is coeval with our record.

695 Thanks to A all these observations, and thanks to the regional comparison with other proxies over the Victoria Land coast, we can advance the hypothesis that Edisto Inlet suggest that, and the TE of the benthic foraminifera in Edisto Inlet can be used a sentinel for changing in the strength of the upwelling of the CDW over the Ross Sea are related to the sea-ice cover variations that, consequently, are connected to the regional oceanographic and atmospheric changes, thus providing an exceptional record that offers high-resolution insight about the environmental changes over the Victoria Land Coast. on the oceanographical and

700 atmospheric changes over this area.

Since the results of the 1.55 kyrs BP (sect. 3.2.6 and sect. 3.2.7) to recent align with the results from the specific benthic foraminiferal analysis reported in Galli et al., (2023), we referred the reader to that article for in depth details while we report a summary of those findings.

In this previous study, by analyzing the *Stainforthia feylingi* and the *Miliammina arenacea* accumulation fluxes, it was possible

705 to recognise the presence of a cospicuous glacial meltwater input. This was connected to the retreat of local glaciers, reflecting milder condition reflecting the onset of MCA (Medieval Climate Anomaly, Lüning et al., (2019)). At 1.2-1.0 kyrs BP (Fig. 6) The TE is characterized by the changes in from a calcareous dominated assemblage to an agglutinated one (Fig. 5). This happens in conjunction with a sudden decrease in the primary productivity proxy (Fig. 5c,d,f,g). Ice cores retrieved over the Victoria Land Coast also reported this sudden decrease of the atmospheric temperature of about -2°C around 1.1 kyrs BP

710 (Mezgec et al., 2017; Stenni et al., 2017). Hence, the presence of this TE it is probably related to an increase in the sea-ice duration over the summer season, reflecting a regional change.

The Last 0.7 kyrs BP period is characterised by the lowest fluxes of accumulation of the benthic foraminifera, that might be caused by an increase in the harsher condition that prevails over the benthic foraminiferal community, probably reflecting the onset of the Little Ice Age (LIA, (Rhodes et al., 2012; Stenni et al., 2017)).

4 Conclusion

In this study we analysed the environmental shifts inferred on the Edisto Inlet ~~using the marine sediment core TR17-08. In addition, we use~~ by looking at the the Rate-of-Change (RoC) analysis on the benthic foraminiferal assemblage to infer significant environmental shifts. We showed that the RoC could bear relevant information for paleoenviromental reconstruction. ~~that occurred at the local level~~. Four different ~~environmental shifts~~Turnover Event (TE) ~~on~~ the benthic foraminiferal community were recognised: 3.3-3.1 kyrs BP, 2.5-2.7 kyrs BP, 1.2 – 1.0 kyrs BP and 0.7 kyrs BP. While the first ~~one can~~did not have any long-term effect ~~be regarded as a not a consequence of a~~on the faunal composition,~~long-lasting change in the environment,~~ the other three TE ~~can be connected~~were caused by ~~to~~ major environmental changes that had long-term effect on the faunal composition. ~~some effect on the assemblage composition.~~ In Edisto Inlet, changes in the RoC values are indicative of different sea-ice cover regimes. Of particular interest, ~~The~~ the TE at 2.7-2.5~~7~~ kyrs BP was caused by ~~is connected ~~a~~to a transition from a multi-year sea-ice dominated environment (3.6-2.7 kyrs BP) to a seasonal sea-ice dominated one (2.5-1.2 kyrs BP). The presence of this change in the sea-ice type in the fjord had the effect of increasing the stability of the benthic community, resulting in more stable community over the seasonal sea-ice phase.~~, with~~ The loss of *Miliammina arenacea* and *Trifarina angulosa* in conjunction with increases in *Epistominella exigua*. ~~Integrating these significant turnover event in conjunction with the geochemical proxies derived from,~~ suggested more intrusion of mCDW (modified Circumpolar Deep Water) over the 2.5-1.2 kyrs BP period. XRF ratio (Zr/Rb, Br/Ti and Ca/Ti) showed a good agreement with the benthic record, demonstrating the potentiality of using RoC analysis in paleoenvironmental studies to identify important faunal changes that are connected to environmental transitions~~demonstrating the potentiality of the RoC analysis in local paleoenvironmental studies to depict a comprehensive view of the environmental evolution of an area.~~ ~~To understand what caused this transition, we compare our results to~~ By looking at a more regional setting, the seasonal sea-ice phase (2.5-1.5 kyrs BP) is coeval with the ~~changing inferring~~ over the Victoria Land Coast, with a similar type of sea-ice change occurring over the same interval. The presence of positive summer phases of the Southern Annular Mode during this period strengthens this view, with more upwelling of CDW onto the shelf and increasing polynya efficiency.

~~other Victoria Land Coast proxies. By doing that, we successfully connected the local changes to intrusion of mCDW on the region, strengthening after the 2.7-2.5 kyrs BP. The TE at 1.2-1.0 kyrs BP it relates to increasing dissolution condition, as testify by the switch from a calcareous to an agglutinated dominated one, probably connected to a period of major atmospheric cooling happening over the Victoria Land coast. Consequently, the 0.7 kyrs BP TE event can be connected to change in sedimentation rate, probably related to the Little Ice Age.~~

Lastly, we ~~stressed~~ highlight~~out~~ the importance that ~~this site~~ Edisto Inlet might~~could~~ have to ~~infer~~study regional oceanographical changes over the Ross Sea region, implying that the ~~Edisto Inlet~~ local enviromental transitions that this site experience ~~could~~ can~~be used as a sentinel for the ~~whole~~ changing over the Victoria Land Region. Thus, the presence of this high-resolution record could offer key insights on the Holocene environmental ~~evolution at very short time scales~~over the Ross Sea.

ha formattato: Tipo di carattere: Corsivo

5 Data availability

All the data used in this study are included in the supplementary material of this article.

6 Author contributions

GG: conceptualization, formal analysis, investigation, visualization, writing the original draft and preparation; KHH: formal analysis, investigation, validation; AdR, FG and PG: data curation; AdR and KG: Funding acquisition. All authors contributed to the reviewing and editing process.

7 Competing interests

The authors declare that they have no conflict of interests.

8 Acknowledgemnts

We thank the sorting centre of MNA – Trieste (Italy) for the sediment core samples, and the CNR-ISMAR section of Bologna (Italy) for the XRF core scanning analysis and data. We also thank all the staff of the R/V Laura BassiItalica, and the dr. Leonardo Langone for his contributions to sample campaign and the radiocarbon dating.

9 Financial support

This research has been supported by the Ministero dell'Università e della Ricerca (projects EDISTHO (grant no. PNRA 2018_00010) and TRACERS (grant no. PNRA2016A3/00055)).

10 References

Allen, C. S. and Weich, Z. C.: Variety and Distribution of Diatom-Based Sea Ice Proxies in Antarctic Marine Sediments of the Past 2000 Years, Geosciences (Basel), 12, 282, https://doi.org/10.3390/geosciences12080282, 2022.

Anderson, J. B.: Ecology and Distribution of Foraminifera in the Weddel Sea of Antarctica, Micropaleontology, 21, 69–96, https://doi.org/10.2307/1485156, 1975.

Arrigo, K. R. and van Dijken, G. L.: Annual changes in sea-ice, chlorophyll a, and primary production in the Ross Sea, Antarctica, Deep Sea Research Part II: Topical Studies in Oceanography, 51, 117–138, https://doi.org/10.1016/j.dsr2.2003.04.003, 2004.

Bart, P. J., DeCesare, M., Rosenheim, B. E., Majewski, W., and McGlannan, A.: A centuries-long delay between a paleo-ice-shelf collapse and grounding-line retreat in the Whales Deep Basin, eastern Ross Sea, Antarctica, Sci Rep, 8, 12392, https://doi.org/10.1038/s41598-018-29911-8, 2018.

775 Battaglia, F., De Santis, L., Baradello, L., Colizza, E., Rebesco, M., Kovacevic, V., Ursella, L., Bensi, M., Accettella, D., Morelli, D., Corradi, N., Falco, P., Krauzig, N., Colleoni, F., Gordini, E., Caburlotto, A., Langone, L., and Finocchiaro, F.: The discovery of the southernmost ultra-high-resolution Holocene paleoclimate sedimentary record in Antarctica, Mar Geol, 467, 107189, https://doi.org/10.1016/j.margeo.2023.107189, 2024.

Belt, S. T., Smik, L., Brown, T. A., Kim, J. H., Rowland, S. J., Allen, C. S., Gal, J. K., Shin, K. H., Lee, J. I., and Taylor, K. W.: Source identification and distribution reveals the potential of the geochemical Antarctic sea ice proxy IPSO25, Nat

780 Commun, 7, 12655, https://doi.org/10.1038/ncomms12655, 2016.

Bernhard, J. M.: Experimental and field evidence of Antarctic foraminiferal tolerance to anoxia and hydrogen sulfide, Mar Micropaleontol, 20, 203–213, https://doi.org/10.1016/0377-8398(93)90033-T, 1993.

Budillon, G., Castagno, P., Aliani, S., Spezie, G., and Padman, L.: Thermohaline variability and Antarctic bottom water formation at the Ross Sea shelf break, Deep Sea Research Part I: Oceanographic Research Papers, 58, 1002–1018,

785 https://doi.org/10.1016/j.dsr.2011.07.002, 2011.

Campbell, E. C., Wilson, E. A., Moore, G. W. K., Riser, S. C., Brayton, C. E., Mazloff, M. R., and Talley, L. D.: Antarctic offshore polynyas linked to Southern Hemisphere climate anomalies, Nature, 570, 319–325, https://doi.org/10.1038/s41586-019-1294-0, 2019.

Capotondi, L., Bergami, C., Giglio, F., Langone, L., and Ravaioli, M.: Benthic foraminifera distribution in the Ross Sea

790 (Antarctica) and its relationship to oceanography, Bollettino della Società Paleontologica Italiana, 57, 187–202, https://doi.org/10.4435/BSPI.2018.12, 2018.

Capotondi, L., Bonomo, S., Budillon, G., Giordano, P., and Langone, L.: Living and dead benthic foraminiferal distribution in two areas of the Ross Sea (Antarctica), Rend Lincei Sci Fis Nat, 31, 1037–1053, https://doi.org/10.1007/s12210-020-00949-z, 2020.

795 Carvalho, F., Kohut, J., Oliver, M. J., Sherrell, R. M., and Schofield, O.: Mixing and phytoplankton dynamics in a submarine canyon in the West Antarctic Peninsula, J Geophys Res Oceans, 121, 5069–5083, https://doi.org/10.1002/2016jc011650, 2016.

Castagno, P., Falco, P., Dinniman, M. S., Spezie, G., and Budillon, G.: Temporal variability of the Circumpolar Deep Water inflow onto the Ross Sea continental shelf, Journal of Marine Systems, 166, 37–49, https://doi.org/10.1016/j.jmarsys.2016.05.006, 2017.

800 Christ, A. J., Talaia-Murray, M., Elking, N., Domack, E. W., Leventer, A., Lavoie, C., Brachfeld, S., Yoo, K. C., Gilbert, R., Jeong, S. M., Petrushak, S., Wellner, J., Balco, G., Brachfeld, S., de Batist, M., Domack, E., Gordon, A., Haran, A., Henriet, J. P., Huber, B., Ishman, S., Jeong, S., King, M., Lavoie, C., Leventer, A., McCormick, M., Mosley-Thompson, E., Pettit, E., Scambos, T., Smith, C., Thompson, L., Truffer, M., van Dover, C., Vernet, M., Wellner, J., Yu, K., and Zagorodnov, V.: Late

Holocene glacial advance and ice shelf growth in Barilari Bay, Graham Land, West Antarctic Peninsula, Bulletin of the
805   Geological Society of America, 127, 297–315, https://doi.org/10.1130/B31035.1, 2015.

Dale, E. R., McDonald, A. J., Coggins, J. H. J., and Rack, W.: Atmospheric forcing of sea ice anomalies in the Ross Sea polynya region, Cryosphere, 11, 267–280, https://doi.org/10.5194/tc-11-267-2017, 2017.

Dinniman, M. S., Klinck, J. M., and Smith, W. O.: A model study of Circumpolar Deep Water on the West Antarctic Peninsula and Ross Sea continental shelves, Deep Sea Res 2 Top Stud Oceanogr, 58, 1508–1523,
810   https://doi.org/10.1016/j.dsr2.2010.11.013, 2011.

Drucker, R., Martin, S., and Kwok, R.: Sea ice production and export from coastal polynyas in the Weddell and Ross Seas, Geophys Res Lett, 38, n/a-n/a, https://doi.org/10.1029/2011gl048668, 2011.

Duffield, C. J., Hess, S., Norling, K., and Alve, E.: The response of Nonionella iridea and other benthic foraminifera to "fresh" organic matter enrichment and physical disturbance, Mar Micropaleontol, 120, 20–30,
815   https://doi.org/10.1016/j.marmicro.2015.08.002, 2015.

Emslie, S. D., Berkman, P. A., Ainley, D. G., Coats, L., and Polito, M.: Late-Holocene initiation of ice-free ecosystems in the southern Ross Sea, Antarctica, Mar Ecol Prog Ser, 262, 19–25, https://doi.org/10.3354/meps262019, 2003.

Emslie, S. D., McKenzie, A., and Patterson, W. P.: The rise and fall of an ancient adélie penguin 'supercolony' at cape adare, antarctica, R Soc Open Sci, 5, https://doi.org/10.1098/rsos.172032, 2018.

820   Finocchiaro, F., Langone, L., Colizza, E., Fontolan, G., Giglio, F., and Tuzzi, E.: Record of the early Holocene warming in a laminated sediment core from Cape Hallett Bay (Northern Victoria Land, Antarctica), Glob Planet Change, 45, 193–206, https://doi.org/10.1016/j.gloplacha.2004.09.003, 2005.

Fogt, R. L. and Marshall, G. J.: The Southern Annular Mode: Variability, trends, and climate impacts across the Southern Hemisphere, https://doi.org/10.1002/wcc.652, 1 July 2020.

825   Forsch, K. O., Hahn-Woernle, L., Sherrell, R. M., Roccanova, V. J., Bu, K., Burdige, D., Vernet, M., and Barbeau, K. A.: Seasonal dispersal of fjord meltwaters as an important source of iron and manganese to coastal Antarctic phytoplankton, Biogeosciences, 18, 6349–6375, https://doi.org/10.5194/bg-18-6349-2021, 2021.

Foster, D. R., KSchoonmaker, P., and Pickett, S. T. A.: Insights from paleoecology to community ecology, Trends Ecol Evol, 5, 119–122, https://doi.org/10.1016/0169-5347(90)90166-B, 1990.

830   Fraser, A. D., Wongpan, P., Langhorne, P. J., Klekociuk, A. R., Kusahara, K., Lannuzel, D., Massom, R. A., Meiners, K. M., Swadling, K. M., Atwater, D. P., Brett, G. M., Corkill, M., Dalman, L. A., Fiddes, S., Granata, A., Guglielmo, L., Heil, P., Leonard, G. H., Mahoney, A. R., McMinn, A., van der Merwe, P., Weldrick, C. K., and Wienecke, B.: Antarctic Landfast Sea Ice: A Review of Its Physics, Biogeochemistry and Ecology, https://doi.org/10.1029/2022RG000770, 1 June 2023.

Galli, G., Morigi, C., Melis, R., Di Roberto, A., Tesi, T., Torricella, F., Langone, L., Giordano, P., Colizza, E., Capotondi, L.,
835   Gallerani, A., and Gariboldi, K.: Paleoenvironmental changes related to the variations of the sea-ice cover during the Late Holocene in an Antarctic fjord (Edisto Inlet, Ross Sea) inferred by foraminiferal association, J Micropalaeontol, 42, 95–115, https://doi.org/10.5194/jm-42-95-2023, 2023.

Galli, G., Morigi, C., Thuy, B., and Gariboldi, K.: Late Holocene echinoderm assemblages can serve as paleoenvironmental tracers in an Antarctic fjord, Sci Rep, 14, https://doi.org/10.1038/s41598-024-66151-5, 2024.

840 Gordon, A. L., Visbeck, M., and Comiso, J. C.: A Possible Link between the Weddell Polynya and the Southern Annular Mode*, J Clim, 20, 2558–2571, https://doi.org/10.1175/JCLI4046.1, 2007.

Grange, L. J., Tyler, P. A., Peck, L., and Cornelius, N.: Long-term interannual cycles of the gametogenic ecology of the Antarctic brittle star Ophionotus victoriae, Mar Ecol Prog Ser, 278, 14–155, https://doi.org/10.3354/meps278141, 2004.

Sen Gupta, B. K.: Modern Foraminifera, Springer Netherlands, Dordrecht, https://doi.org/10.1007/0-306-48104-9, 2003.

845 Hall, B. L., Hoelzel, A. R., Baroni, C., Denton, G. H., Le Boeuf, B. J., Overturf, B., and Topf, A. L.: Holocene elephant seal distribution implies warmer-than-present climate in the Ross Sea, PNAS, 103, 10213–10217, https://doi.org/10.1073/pnas.0604002103, 2006.

Hall, B. L., Koch, P. L., Baroni, C., Salvatore, M. C., Hoelzel, A. R., de Bruyn, M., and Welch, A. J.: Widespread southern elephant seal occupation of the Victoria land coast implies a warmer-than-present Ross Sea in the mid-to-late Holocene, Quat

850 Sci Rev, 303, https://doi.org/10.1016/j.quascirev.2023.107991, 2023.

Hansen, K. E., Pearce, C., and Seidenkrantz, M. S.: Response of Arctic benthic foraminiferal traits to past environmental changes, Sci Rep, 13, https://doi.org/10.1038/s41598-023-47603-w, 2023.

Harloff, J. and Mackensen, A.: Recent benthic foraminiferal associations and ecology of the Scotia Sea and Argentin Basin, Mar Micropaleontol, 31, 1–29, https://doi.org/10.1016/S0377-8398(96)00059-X, 1997.

855 Herguera, J. C. and Berger, W. H.: Paleoproductivity from benthic foraminifera abundance: Glacial to postglacial change in the west-equatorial Pacific, Geology, 19, 1173–1176, https://doi.org/10.1130/0091-7613(1991)019<1173:PFBFAG>2.3.CO;2, 1991.

Howe, J. A., Austin, W. E. N., Forwick, M., Paetzel, M., Harland, R., and Cage, A. G.: Fjord systems and archives: a review, Geological Society, London, Special Publications, 344, 5–15, https://doi.org/10.1144/sp344.2, 2010.

860 Igarashi, A., Numanami, H., Tsuchiya, Y., and Fukuchi, M.: Bathymetric distribution of fossil foraminifera within marine sediment cores from the eastern part of Lützow-Holm Bay, East Antarctica, and its paleoceanographic implications, Mar Micropaleontol, 42, 125–162, https://doi.org/10.1016/S0377-8398(01)00004-4, 2001.

Ishman, S. E. and Sperling, M. R.: Benthic foraminiferal record of Holocene deep-water evolution in the Palmer Deep, western Antarctica Peninsula, Geology, 30, 435–438, https://doi.org/10.1130/0091-7613(2002)030<0435:BFROHD>2.0.CO;2, 2002.

865 Ishman, S. E. and Szymcek, P.: Foraminiferal Distributions in the Former Larsen-A Ice Shelf and Prince Gustav Channel Region, Eastern Antarctic Peninsula Margin: A Baseline for Holocene Paleoenvironmental Change, in: Antarctic Peninsula Climate Variability: Historical and Paleoenvironmental Perspectives, 239–260, https://doi.org/10.1029/AR079p0239, 2003.

Jacobson, G. L. and Grimm, E. C.: A Numerical Analysis of Holocene Forest and Prairie Vegetation in Central Minnesota, Ecology, 67, 958–966, https://doi.org/10.2307/1939818, 1986.

870 Knudsen, K. L., Stabell, B., Seidenkrantz, M.-S., EirÍKsson, J. Ó. N., and Blake, W.: Deglacial and Holocene conditions in northernmost Baffin Bay: sediments, foraminifera, diatoms and stable isotopes, Boreas, 37, 346–376, https://doi.org/10.1111/j.1502-3885.2008.00035.x, 2008.

Korsun, S., Kniazeva, O., Majewski, W., Godoi, M. A., Hromic, T., Varfolomeeva, M., and Pawlowski, J.: Foraminifera in temperate fjords strongly affected by glacial meltwater, Tierra del Fuego, South America, Mar Micropaleontol, 181,
875 https://doi.org/10.1016/j.marmicro.2023.102248, 2023.

Kyrmanidou, A., Vadman, K. J., Ishman, S. E., Leventer, A., Brachfeld, S., Domack, E. W., and Wellner, J. S.: Late Holocene oceanographic and climatic variability recorded by the Perseverance Drift, northwestern Weddell Sea, based on benthic foraminifera and diatoms, Mar Micropaleontol, 141, 10–22, https://doi.org/10.1016/j.marmicro.2018.03.001, 2018.

Lamy, F., Winckler, G., Arz, H. W., Farmer, J. R., Gottschalk, J., Lembke-Jene, L., Middleton, J. L., van der Does, M.,
880 Tiedemann, R., Alvarez Zarikian, C., Basak, C., Brombacher, A., Dumm, L., Esper, O. M., Herbert, L. C., Iwasaki, S., Kreps, G., Lawson, V. J., Lo, L., Malinverno, E., Martinez-Garcia, A., Michel, E., Moretti, S., Moy, C. M., Ravelo, A. C., Riesselman, C. R., Saavedra-Pellitero, M., Sadatzki, H., Seo, I., Singh, R. K., Smith, R. A., Souza, A. L., Stoner, J. S., Toyos, M., de Oliveira, I. M. V. P., Wan, S., Wu, S., and Zhao, X.: Five million years of Antarctic Circumpolar Current strength variability, Nature, 627, 789–796, https://doi.org/10.1038/s41586-024-07143-3, 2024.

885 Leventer, A., Dunbar, R. B., and DeMaster, D. J.: Diatom evidence for Late Holocene climatic events in Granite Harbor, Antarctica, Paleoceanography, 8, 373–386, https://doi.org/10.1029/93PA00561, 1993.

Li, B., Yoon, H., and Park, B.: Foraminiferal assemblages and CaCO3 dissolution since the last deglaciation in the Maxwell Bay, King George Island, Antarctica, Mar Geol, 169, 239–257, https://doi.org/10.1016/S0025-3227(00)00059-1, 2000.

Loeblich, A. R. and Tappan, H.: Foraminiferal Genera and Their Classification, Springer US, Boston, MA,
890 https://doi.org/10.1007/978-1-4899-5760-3, 1988.

Lüning, S., Gałka, M., and Vahrenholt, F.: The Medieval Climate Anomaly in Antarctica, Palaeogeogr Palaeoclimatol Palaeoecol, 532, https://doi.org/10.1016/j.palaeo.2019.109251, 2019.

Majewski, W.: Benthic foraminiferal communities: distribution and ecology in Admiralty Bay, King George Island, West Antarctica, Pol Polar Res, 26, 159–214, 2005.

895 Majewski, W.: Benthic foraminifera from West Antarctic fiord environments: An overview, Pol Polar Res, 31, 61–82, https://doi.org/10.4202/ppres.2010.05, 2010.

Majewski, W.: Supplement of Unique benthic foraminiferal communities (stained) in diverse environments of sub-Antarctic fjords, South Georgia, 20, 523–544, https://doi.org/10.5194/bg-20-523-2023-supplement, 2023.

Majewski, W. and Anderson, J. B.: Holocene foraminiferal assemblages from Firth of Tay, Antarctic Peninsula: Paleoclimate
900 implications, Mar Micropaleontol, 73, 135–147, https://doi.org/10.1016/j.marmicro.2009.08.003, 2009.

Majewski, W., Wellner, J. S., and Anderson, J. B.: Environmental connotations of benthic foraminiferal assemblages from coastal West Antarctica, Mar Micropaleontol, 124, 1–15, https://doi.org/10.1016/j.marmicro.2016.01.002, 2016.

Majewski, W., Bart, P. J., and McGlannan, A. J.: Foraminiferal assemblages from ice-proximal paleo-settings in the Whales Deep Basin, eastern Ross Sea, Antarctica, Palaeogeogr Palaeoclimatol Palaeoecol, 493, 64–81, https://doi.org/10.1016/j.palaeo.2017.12.041, 2018.

Marshall, G. J.: Trends in the Southern Annular Mode from observations and reanalyses, J Clim, 16, 4134–4143, https://doi.org/https://doi.org/10.1175/1520-0442(2003)016<4134:TITSAM>2.0.CO;2, 2003.

Massé, G., Belt, S. T., Crosta, X., Schmidt, S., Snape, I., Thomas, D. N., and Rowland, S. J.: Highly branched isoprenoids as proxies for variable sea ice conditions in the Southern Ocean, Antarct Sci, 23, 487–498, https://doi.org/10.1017/s0954102011000381, 2011.

Mathiot, P., Jourdain, N. C., Barnier, B., Gallée, H., Molines, J. M., Le Sommer, J., and Penduff, T.: Sensitivity of coastal polynyas and high-salinity shelf water production in the Ross Sea, Antarctica, to the atmospheric forcing, Ocean Dyn, 62, 701–723, https://doi.org/10.1007/s10236-012-0531-y, 2012.

Matsuoka, K., Skoglund, A., Roth, G., de Pomereu, J., Griffiths, H., Headland, R., Herried, B., Katsumata, K., Le Brocq, A., Licht, K., Morgan, F., Neff, P. D., Ritz, C., Scheinert, M., Tamura, T., Van de Putte, A., van den Broeke, M., von Deschwanden, A., Deschamps-Berger, C., Van Liefferinge, B., Tronstad, S., and Melvær, Y.: Quantarctica, an integrated mapping environment for Antarctica, the Southern Ocean, and sub-Antarctic islands, Environmental Modelling & Software, 140, https://doi.org/10.1016/j.envsoft.2021.105015, 2021.

Melis, R. and Salvi, G.: Late Quaternary foraminiferal assemblages from western Ross Sea (Antarctica) in relation to the main glacial and marine lithofacies, Mar Micropaleontol, 70, 39–53, https://doi.org/10.1016/j.marmicro.2008.10.003, 2009.

Melis, R., Capotondi, L., Torricella, F., Ferretti, P., Geniram, A., Hong, J. K., Kuhn, G., Khim, B.-K., Kim, S., Malinverno, E., Yoo, K. C., and Colizza, E.: Last Glacial Maximum to Holocene paleoceanography of the northwestern Ross Sea inferred from sediment core geochemistry and micropaleontology at Hallett Ridge, J Micropalaeontol, 40, 15–35, https://doi.org/10.5194/jm-40-15-2021, 2021.

Mezgec, K., Stenni, B., Crosta, X., Masson-Delmotte, V., Baroni, C., Braida, M., Ciardini, V., Colizza, E., Melis, R., Salvatore, M. C., Severi, M., Scarchilli, C., Traversi, R., Udisti, R., and Frezzotti, M.: Holocene sea ice variability driven by wind and polynya efficiency in the Ross Sea, Nat Commun, 8, 1334, https://doi.org/10.1038/s41467-017-01455-x, 2017.

Mottl, O., Flantua, S. G. A., Bhatta, K. P., Felde, V. A., Giesecke, T., Goring, S., Grimm, E. C., Haberle, S., Hooghiemstra, H., Ivory, S., Kuneš, P., Wolters, S., Seddon, A. W. R., and Williams, J. W.: Global acceleration in rates of vegetation change over the past 18,000 years, Science (1979), 372, 860–864, https://doi.org/10.1126/science.abg1685, 2021a.

Mottl, O., Grytnes, J. A., Seddon, A. W. R., Steinbauer, M. J., Bhatta, K. P., Felde, V. A., Flantua, S. G. A., and Birks, H. J. B.: Rate-of-change analysis in paleoecology revisited: A new approach, Rev Palaeobot Palynol, 293, https://doi.org/10.1016/j.revpalbo.2021.104483, 2021b.

Murray, J. W.: Ecology and palaeoecology of benthic foraminifera, Routledge, 1991.

Murray, J. W.: Ecology and Applications of Benthic Foraminifera, Cambridge University Press, https://doi.org/10.1017/CBO9780511535529, 2006.

Murray, J. W. and Pudsey, C. J.: Living (stained) and dead foraminifera from the newly ice-free Larsen Ice Shelf, Weddell Sea, Antarctica: Ecology and taphonomy, Mar Micropaleontol, 53, 67–81, https://doi.org/10.1016/j.marmicro.2004.04.001, 2004.

940 Orsi, A. H. and Wiederwohl, C. L.: A recount of Ross Sea waters, Deep Sea Research Part II: Topical Studies in Oceanography, 56, 778–795, https://doi.org/10.1016/j.dsr2.2008.10.033, 2009.

O'Sullivan, J. D., Terry, J. C. D., and Rossberg, A. G.: Intrinsic ecological dynamics drive biodiversity turnover in model metacommunities, Nat Commun, 12, https://doi.org/10.1038/s41467-021-23769-7, 2021.

Pan, B. J., Vernet, M., Manck, L., Forsch, K., Ekern, L., Mascioni, M., Barbeau, K. A., Almandoz, G. O., and Orona, A. J.:
945 Environmental drivers of phytoplankton taxonomic composition in an Antarctic fjord, Prog Oceanogr, 183, https://doi.org/10.1016/j.pocean.2020.102295, 2020.

Pauling, A. G., Smith, I. J., Langhorne, P. J., and Bitz, C. M.: Time-Dependent Freshwater Input From Ice Shelves: Impacts on Antarctic Sea Ice and the Southern Ocean in an Earth System Model, Geophys Res Lett, 44, 10, 410–454, 461, https://doi.org/10.1002/2017gl075017, 2017.

950 Peck, V. L., Allen, C. S., Kender, S., McClymont, E. L., and Hodgson, D. A.: Oceanographic variability on the West Antarctic Peninsula during the Holocene and the influence of upper circumpolar deep water, Quat Sci Rev, 119, 54–65, https://doi.org/10.1016/j.quascirev.2015.04.002, 2015.

Piva, A., Asioli, A., Schneider, R. R., Trincardi, F., Andersen, N., Colmenero-Hidalgo, E., Dennielou, B., Flores, J. A., and Vigliotti, L.: Climatic cycles as expressed in sediments of the PROMESSI borehole PRAD1-2, central Adriatic, for the last
955 370 ka: 1. Integrated stratigraphy, Geochemistry, Geophysics, Geosystems, 9, https://doi.org/10.1029/2007GC001713, 2008.

Reeh, N., Mayer, C., Miller, H., Thomsen, H. H., and Weidick, A.: Present and past climate control on fjord glaciations in Greenland: Implications for IRD-deposition in the sea, Geophys Res Lett, 26, 1039–1042, https://doi.org/10.1029/1999GL900065, 1999.

Rhodes, R. H., Bertler, N. A. N., Baker, J. A., Steen-Larsen, H. C., Sneed, S. B., Morgenstern, U., and Johnsen, S. J.: Little
960 Ice Age climate and oceanic conditions of the Ross Sea, Antarctica from a coastal ice core record, Climate of the Past, 8, 1223–1238, https://doi.org/10.5194/cp-8-1223-2012, 2012.

Di Roberto, A., Colizza, E., Del Carlo, P., Petrelli, M., Finocchiaro, F., and Kuhn, G.: First marine cryptotephra in Antarctica found in sediments of the western Ross Sea correlates with englacial tephras and climate records, Sci Rep, 9, 10628, https://doi.org/10.1038/s41598-019-47188-3, 2019.

965 Di Roberto, A., Re, G., Scateni, B., Petrelli, M., Tesi, T., Capotondi, L., Morigi, C., Galli, G., Colizza, E., Melis, R., Torricella, F., Giordano, P., Giglio, F., Gallerani, A., and Gariboldi, K.: Cryptotephras in the marine sediment record of the Edisto Inlet, Ross Sea: Implications for the volcanology and tephrochronology of northern Victoria Land, Antarctica, Quaternary Science Advances, 10, https://doi.org/10.1016/j.qsa.2023.100079, 2023.

Rusciano, E., Budillon, G., Fusco, G., and Spezie, G.: Evidence of atmosphere–sea ice–ocean coupling in the Terra Nova Bay
970 polynya (Ross Sea—Antarctica), Cont Shelf Res, 61–62, 112–124, https://doi.org/10.1016/j.csr.2013.04.002, 2013.

Sabbatini, A., Morigi, C., Ravaioli, M., and Negri, A.: Abyssal benthic foraminifera in the Polar Front region (Pacific sector): Faunal composition, standing stock and size structure, Chemistry and Ecology, 20, S117–S129, https://doi.org/10.1080/02757540410001655387, 2004.

Seidenkrantz, M.-S.: Benthic foraminifera as palaeo sea-ice indicators in the subarctic realm – examples from the Labrador Sea–Baffin Bay region, Quat Sci Rev, 79, 135–144, https://doi.org/10.1016/j.quascirev.2013.03.014, 2013.

Seidenstein, J. L., Cronin, T. M., Gemery, L., Keigwin, L. D., Pearce, C., Jakobsson, M., Coxall, H. K., Wei, E. A., and Driscoll, N. W.: Late Holocene paleoceanography in the Chukchi and Beaufort Seas, Arctic Ocean, based on benthic foraminifera and ostracodes, arktos, 4, 1–17, https://doi.org/10.1007/s41063-018-0058-7, 2018.

Shimadzu, H., Dornelas, M., and Magurran, A. E.: Measuring temporal turnover in ecological communities, Methods Ecol Evol, 6, 1384–1394, https://doi.org/10.1111/2041-210X.12438, 2015.

Silvestri, G., Berman, A. L., Braconnot, P., and Marti, O.: Long-term trends in the Southern Annular Mode from transient Mid- to Late Holocene simulation with the IPSL-CM5A2 climate model, Clim Dyn, 59, 903–914, https://doi.org/10.1007/s00382-022-06160-0, 2022.

Simpson, G. L.: Modelling palaeoecological time series using generalised additive models, Front Ecol Evol, 6, https://doi.org/10.3389/fevo.2018.00149, 2018.

Smith Jr., W. O., Ainley, D. G., Arrigo, K. R., and Dinniman, M. S.: The oceanography and ecology of the Ross Sea, Ann Rev Mar Sci, 6, 469–487, https://doi.org/10.1146/annurev-marine-010213-135114, 2014.

Smith, W., Sedwick, P., Arrigo, K., Ainley, D., and Orsi, A.: The Ross Sea in a Sea of Change, Oceanography, 25, 90–103, https://doi.org/10.5670/oceanog.2012.80, 2012.

Smith, W. O. and Gordon, L. I.: Hyperproductivity of the Ross Sea (Antarctica) polynya during austral spring, Geophys Res Lett, 24, 233–236, https://doi.org/10.1029/96gl03926, 1997.

Stenni, B., Curran, M. A. J., Abram, N. J., Orsi, A., Goursaud, S., Masson-Delmotte, V., Neukom, R., Goosse, H., Divine, D., van Ommen, T., Steig, E. J., Dixon, D. A., Thomas, E. R., Bertler, N. A. N., Isaksson, E., Ekaykin, A., Werner, M., and Frezzotti, M.: Antarctic climate variability on regional and continental scales over the last 2000 years, Climate of the Past, 13, 1609–1634, https://doi.org/10.5194/cp-13-1609-2017, 2017.

Strugnell, J. M., McGregor, H. V., Wilson, N. G., Meredith, K. T., Chown, S. L., Lau, S. C. Y., Robinson, S. A., and Saunders, K. M.: Emerging biological archives can reveal ecological and climatic change in Antarctica, https://doi.org/10.1111/gcb.16356, 1 November 2022.

Taylor, S. P., Patterson, M. O., Lam, A. R., Jones, H., Woodard, S. C., Habicht, M. H., Thomas, E. K., and Grant, G. R.: Expanded North Pacific Subtropical Gyre and Heterodyne Expression During the Mid-Pleistocene, Paleoceanogr Paleoclimatol, 37, https://doi.org/10.1029/2021PA004395, 2022.

Tesi, T., Belt, S. T., Gariboldi, K., Muschitiello, F., Smik, L., Finocchiaro, F., Giglio, F., Colizza, E., Gazzurra, G., Giordano, P., Morigi, C., Capotondi, L., Nogarotto, A., Köseoğlu, D., Di Roberto, A., Gallerani, A., and Langone, L.: Resolving sea ice

dynamics in the north-western Ross Sea during the last 2.6 ka: From seasonal to millennial timescales, Quat Sci Rev, 237,

1005   https://doi.org/10.1016/j.quascirev.2020.106299, 2020.

Tomašových, A. and Kidwell, S. M.: The effects of temporal resolution on species turnover and on testing metacommunity models, American Naturalist, 175, 587–606, https://doi.org/10.1086/651661, 2010.

Toyos, M. H., Lamy, F., Lange, C. B., Lembke-Jene, L., Saavedra-Pellitero, M., Esper, O., and Arz, H. W.: Antarctic Circumpolar Current Dynamics at the Pacific Entrance to the Drake Passage Over the Past 1.3 Million Years, Paleoceanogr

1010   Paleoclimatol, 35, https://doi.org/10.1029/2019pa003773, 2020.

Violanti, D.: Morphogroup Analysis of Recent Agglutinated Foraminifers off Terra Nova Bay, Antarctica (Expedition 1987– 1988), Ross Sea Ecology, 479–492, https://doi.org/10.1007/978-3-642-59607-0_34, 2000.

Wang, Y., Zhou, M., Zhang, Z., and Dinniman, M. S.: Seasonal variations in Circumpolar Deep Water intrusions into the Ross Sea continental shelf, Front Mar Sci, 10, https://doi.org/10.3389/fmars.2023.1020791, 2023.

1015   Waters, R. L., van den Enden, R., and Marchant, H. J.: Summer microbial ecology off East Antarctica (80–150°E): protistan community structure and bacterial abundance, Deep Sea Research Part II: Topical Studies in Oceanography, 47, 2401–2435, https://doi.org/10.1016/S0967-0645(00)00030-8, 2000.

Whitworth, T. and Orsi, A. H.: Antarctic Bottom Water production and export by tides in the Ross Sea, Geophys Res Lett, 33, https://doi.org/10.1029/2006gl026357, 2006.

1020   Wongpan, P., Meiners, K. M., Vancoppenolle, M., Fraser, A. D., Moreau, S., Saenz, B. T., Swadling, K. M., and Lannuzel, D.: Gross Primary Production of Antarctic Landfast Sea Ice: A Model-Based Estimate, J Geophys Res Oceans, 129, https://doi.org/10.1029/2024JC021348, 2024.

Wood Simon: mgcv: GAMs and generalized ridfe regression for R, R news, 1, 20–25, 2001.

Wu, L., Wang, R., Krijgsman, W., Chen, Z., Xiao, W., Ge, S., and Wu, J.: Deciphering Color Reflectance Data of a 520-kyr

1025   Sediment Core From the Southern Ocean: Method Application and Paleoenvironmental Implications, Geochemistry, Geophysics, Geosystems, 20, 2808–2826, https://doi.org/10.1029/2019GC008212, 2019.

Wu, L., Wilson, D. J., Wang, R., Yin, X., Chen, Z., Xiao, W., and Huang, M.: Evaluating Zr/Rb Ratio From XRF Scanning as an Indicator of Grain-Size Variations of Glaciomarine Sediments in the Southern Ocean, Geochemistry, Geophysics, Geosystems, 21, https://doi.org/10.1029/2020GC009350, 2020.

1030   Xu, Q. B., Yang, L. J., Gao, Y. S., Sun, L. G., and Xie, Z. Q.: 6,000-Year Reconstruction of Modified Circumpolar Deep Water Intrusion and Its Effects on Sea Ice and Penguin in the Ross Sea, Geophys Res Lett, 48, https://doi.org/10.1029/2021GL094545, 2021.

Yokoyama, Y., Anderson, J. B., Yamane, M., Simkins, L. M., Miyairi, Y., Yamazaki, T., Koizumi, M., Suga, H., Kusahara, K., Prothro, L., Hasumi, H., Southon, J. R., and Ohkouchi, N.: Widespread collapse of the Ross Ice Shelf during the late

1035   Holocene, Proc Natl Acad Sci U S A, 113, 2354–2359, https://doi.org/10.1073/pnas.1516908113, 2016.

Zhang, Z., Xie, C., Castagno, P., England, M. H., Wang, X., Dinniman, M. S., Silvano, A., Wang, C., Zhou, L., Li, X., Zhou, M., and Budillon, G.: Evidence for large-scale climate forcing of dense shelf water variability in the Ross Sea, Nat Commun, 15, 8190, https://doi.org/10.1038/s41467-024-52524-x, 2024.

Zhou, Y., McManus, J. F., Jacobel, A. W., Costa, K. M., Wang, S., and Alvarez Caraveo, B.: Enhanced iceberg discharge in the western North Atlantic during all Heinrich events of the last glaciation, Earth Planet Sci Lett, 564, https://doi.org/10.1016/j.epsl.2021.116910, 2021.

Ziegler, M., Jilbert, T., De Lange, G. J., Lourens, L. J., and Reichart, G. J.: Bromine counts from XRF scanning as an estimate of the marine organic carbon content of sediment cores, Geochemistry, Geophysics, Geosystems, 9, https://doi.org/10.1029/2007GC001932, 2008.